



Dr. John Runciman Ph.D., P.Eng  
Associate Director of Undergraduate Studies  
50 Stone Rd E,  
Guelph, ON  
N1G 2W1  
THRN 2408

Dear Dr. Runciman,

Please find attached the final report “FSAE Rim Design”. This report outlines the design and fabrication of carbon fibre rims for the Gryphon Racing FSAE team. Should you have any questions regarding this report, please contact us by email at [millero@uoguelph.ca](mailto:millero@uoguelph.ca).

Sincerely,

Nicolas Bessay-Torfs

A handwritten signature in black ink.

Orion Miller

A handwritten signature in black ink.

Andrew Roberts

A handwritten signature in black ink.

Nicole Smith

A handwritten signature in black ink.



## **FSAE Rim Design**

Advisor: Dr. John Runciman Ph.D., P.Eng

Group# 26:

Nicolas Bessay-Torfs

Orion Miller

Andrew Roberts

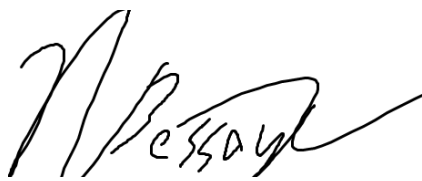
Nicole Smith

April 8<sup>th</sup>, 2019.

*In signing this report and providing my PEO SMP (Student Membership Program) number, I certify that I have been an active member of the team and provided approximately equal contribution to the work. I take shared credit and responsibility for the content of this report. I understand that taking credit for work that is not my own is a form of academic misconduct and will be treated as such.*

**Nicolas Bessay-Torfs**

Team Member One Name



**054284**

Team Member One Signature

Team Member One SMP#

**Orion Miller**

Team Member Two Name



**063296**

Team Member Two Signature

Team Member Two SMP#

**Andrew Roberts**

Team Member Three Name



**059029**

Team Member Three Signature

Team Member Three SMP#

**Nicole Smith**

Team Member Four Name



**054671**

Team Member Four Signature

Team Member Four SMP#

## EXECUTIVE SUMMARY

---

This report outlines efforts to develop a prototype carbon fibre rim design for FSAE racing. This design has been pursued with the goal of improving vehicle performance through reduction in rim mass. The project aims to lay all relevant design groundwork for implementing this change, as well as establish and document suitable manufacturing processes.

The first section reintroduces the problem description and background which has been revised and expanded upon since the interim report. The potential benefits of reducing the mass of the FSAE car's rims are discussed; this includes reduced overall mass and unsprung mass, reduced rotational inertia, and reduced yaw inertia. The combination of these reductions improves acceleration and cornering responsiveness, as well as decreasing weight transfer, all of which are very desirable results for an FSAE car. In this section the forces encountered by the rim under racing conditions are specified. A review of the state of current racing rim technology is conducted. The benefits of carbon fibre compared to magnesium and aluminum rims are discussed. Carbon fibre is a desirable material for a racing rim because it is lighter than magnesium and aluminum alloys while providing much more stiffness and strength (Young's modulus of 228 GPa compared to 45 GPa for magnesium and 70 GPa for aluminum, ultimate tensile strength of 560MPa). An overview of available fibre weaves is conducted. For this project, 2x2 twill weave has been selected in the interest of cost saving, as its properties are suitable and it is already used in other sections of the 2019 car.

The design of the rim, its structural analysis using ANSYS, the design of the mold, and progress developing the layup process are detailed in Section 2. Material testing was done to ensure that ANSYS material properties were reasonable. By finding ultimate tensile strength using an Instron machine, it was possible to verify the quality of materials being used and the potential validity of the designed layup procedure. A 2-degree draft angle was added to the design of the inside shell's profile in order to ensure release from the mold. A female mold was selected as this would ensure that tire bead geometry and other critical surfaces are accurate. The final mold design and the process of manufacturing it is detailed. It was machined in eight parts which assembled to form the complete mold. ANSYS simulations were performed and the resulting deflections and stresses for an aluminum rim and a 10-layer CF rim are compared when subjected to four loading cases: maximum lateral force, maximum longitudinal, maximum normal, and high pressure. The finite element analysis of the designed carbon fibre rim shows that its strength is an improvement over the aluminum rim. The increased wheel offset reduced the benefit of the carbon fibre's higher stiffness and increased deflection at the tire bead. A 10-layer CF rim with this design is estimated to have 50% of the stiffness of the aluminum rim with 17% reduction in mass. This estimate is conservative, and the stiffness to weight ratio may be improved in the future with better CF layups.

The success of this project has been measured by the ability to carry out a comprehensive rim design process, as well as manufacture a full mold assembly and prototype rim to prove the feasibility of the design. During the period of this project, skills such as vehicle dynamics and MATLAB, materials testing, structural analysis and ANSYS, solid modeling, and manufacturing were applied to cover all relevant aspects of this engineering problem. With the successful execution of the intended goals, this project is now considered complete.

## **ACKNOWLEDGEMENTS:**

---

Special thanks to Dr. Runciman Ph.D., P.Eng, Barry Verspagen, Ken Graham, Dave Wright, Gryphon Racing, Anthony Meola, and Musashi Auto Parts.

## **TABLE OF CONTENTS**

---

Executive Summary.....	4
Acknowledgements:.....	5
List of Tables .....	5
List of Figures .....	6
List of Acronyms and Terms.....	7
1.0 Introduction.....	7
1.1 Problem Description .....	8
1.2 Background Information .....	10
1.3 Literature Review .....	15
1.4 Scope and Objectives .....	17
1.5 Constraints and Criteria .....	18
1.6 Project Management .....	19
2.0 Design Methodology.....	21
2.1 Rim Design .....	21
2.2 Mold Design .....	29
2.3 Carbon Layup Process and Prototype.....	34
3.0 Uncertainties and Risk .....	39
4.0 Conclusions and Recommendations.....	40
5.0 References .....	42
6.0 Appendices.....	43
7.0 Resources.....	59
7.1 Bill of Materials and Equipment .....	59

## **LIST OF TABLES**

---

Table 1: Sensitivity Analysis .....	30
-------------------------------------	----

## LIST OF FIGURES

---

Figure 1: Suspension Geometry of GRC19 .....	9
Figure 2: Example of Positive Camber in Cornering Due to Suspension Compliance.....	10
Figure 3: Standard Convention for Forces Acting on a Wheel.....	11
Figure 4: Normal Load due to Lateral Forces and Slip Angle (Tire Deformation) at 10psi .....	12
Figure 5: Maximum Normal Force on One Wheel.....	13
Figure 6: Traction Circle for 1100N Vertical Force.....	14
Figure 7: Tire Temperatures during Lateral Test .....	14
Figure 8: Updated Gantt Chart.....	20
Figure 9: Stress Strain Curves 5- and 10-layer Carbon Fibre Samples .....	21
Figure 10: Machined ASTM 370 Tensile Test Sample .....	22
Figure 11: Comparison of Finalized Rim Profile (Blue) vs. Aluminum Original (Gray) .....	23
Figure 12: Thickness (m) of Inner Shell with 10 layers and 10 Reinforcing Layers (Red Areas) .....	24
Figure 13: Thickness (m) of Outer Shell with 10 layers and 10 Reinforcing Layers (Red Areas) .....	25
Figure 14: Loads and Fixtures. ....	26
Figure 15: Deformation Comparison. ....	27
Figure 16: Stress Comparison. ....	28
Figure 17: Isometric Views of Final Mold Design .....	29
Figure 18: Exploded Final Mold Design.....	30
Figure 19: Mold Assembly Cross Section .....	31
Figure 20: Mold Assembly Isometric View (Displayed Translucent for Detail).....	32
Figure 21: Carbon Fibre Layup Schematic.....	34
Figure 22: Carbon Fibre Test Piece Using a Safety Hat as a Mold .....	35
Figure 23: Banded-style layup shapes. ....	36
Figure 24: Banded-Style Layup in Progress on the Mold .....	36
Figure 25: Radial Slice-Style Layup Shapes. ....	37
Figure 26: Radial-Style Layup in Progress on the Mold. ....	37
Figure 27: Features to be Machined .....	38
Figure 28: Final Prototype.....	39
Figure 29: Rim Profile of Final Design .....	43
Figure 30: Rim Profile of Original Aluminum Design .....	43
Figure 31: Section View of Mold Version 1.....	44
Figure 32: Section View of Mold Version 2 .....	44
Figure 33: Sketched Layout of Fastening Features (Version 2).....	45
Figure 34: CAD Layout of Fastening Features (Version 2) .....	45
Figure 35: Diagram of Mold Removal Using a Hydraulic Press .....	46
Figure 36: Diagram of Section Separation .....	46
Figure 37: Band Saw Cuts to be made in Aluminum Block .....	47
Figure 38: Machining Setup for Machining of Block Side Faces .....	47
Figure 39: Machining of Block Side Faces.....	48
Figure 40: Main Sections after Facing .....	48
Figure 41: Roughing Tool Path for Section 2.....	49
Figure 42: Finishing Tool Path for Section 2 .....	49

Figure 43: Section 2 after CNC Machining .....	50
Figure 44: Section 4 before CNC Machining, with Section 3 and Section 2 Below.....	50
Figure 45: Mold Sections after CNC Machining .....	51
Figure 46: Mold Release of Finished Outer Shell.....	51
Figure 47: Fully Assembled Mold in 3D.....	52
Figure 48: Fully Assembly Mold in 2D.....	53
Figure 49: Schematic of Mold Section 1 .....	54
Figure 50: Schematic of Mold Section 2 .....	55
Figure 51: Schematic of Mold Section 3 .....	56
Figure 52: Schematic of Mold Section 4 .....	57
Figure 53: Schematic of Side Handles.....	58

## LIST OF ACRONYMS AND TERMS

---

FOS – Factor of Safety  
 SOE – School of Engineering (University of Guelph)  
 FSAE - Formula Society of Automotive Engineers  
 GRCxx – Gryphon Race Car (Naming Convention for Gryphon Racing Vehicles)  
 CNC - Computer Numerical Control  
 AML – Advanced Manufacturing Laboratory  
 FEA – Finite Element Analysis  
 ACP - ANSYS Composite Prep/Post  
 PVA – Poly Vinyl Alcohol  
 HSS – High-Speed Steel  
 BOM – Bill of Materials  
 CF – Carbon Fibre

## 1.0 INTRODUCTION

---

41XX design projects are completed by all University of Guelph undergraduate engineering students throughout their final academic year. These projects are meant to challenge students with open-ended design problems and expose them to the types of project planning and management situations that will be encountered during their careers. Students are required to cap their undergraduate degree by bringing together and applying a wide variety of skills, techniques, and tools learned throughout their studies. The 41XX design project is also an opportunity for students to look forward to the types of careers they wish to pursue. This is a chance to gear studies towards fields of interest and learn from working engineers prior to graduation.

This design project focuses on the design and manufacturing of carbon fibre racing rims, in cooperation with the Gryphon Racing Formula SAE team. Formula SAE is an intercollegiate engineering design competition in which teams design, build, and race open-wheel race cars. As the team's size and available resources have increased in recent years, it has become possible for more comprehensive design solutions to be implemented in favor of simple or off-the-shelf parts. However, as time is the

most critical resource to the success of the team, the resulting functional improvements must be quantitatively proven as worthwhile.

Creating carbon fibre components is a highly specialized, time intensive process that is being used with increasing prevalence in automotive applications requiring high performance. When well executed, carbon fibre parts have an unmatched combination of high specific strength and stiffness. It is expected that a significant reduction in mass of the rims can be achieved through this approach, yielding major performance benefits to the Gryphon Racing car. The project therefore aims to lay all the relevant design groundwork for this change, as well as establish and document the required manufacturing processes.

This project has involved the application of skills in vehicle dynamics and MATLAB, materials science, structural analysis and ANSYS, solid modeling, and manufacturing to the problem of developing race-worthy carbon fibre rims. The team has relevant background in these areas, and has also been able to learn new skills, such as carbon fibre layup and vacuum bagging.

## 1.1 PROBLEM DESCRIPTION

---

Before beginning the design process, the specific problems to be addressed by this project should first be examined. The motivation for developing carbon fibre rims to replace the current aluminum rims, which are both affordable and readily available, must have clear justification. The benefits of reduced mass and increased stiffness, the two main improvements possible with this new design, are now explored.

### Impact of Rim Mass on Vehicle Performance

In a racecar, the performance of the vehicle is limited by the mass of the rims for a number of reasons. Firstly, heavier rims have higher rotational inertia, making them more difficult to accelerate about the spindle axis and steering axis (see Figure 1 below). Secondly, the rims are part of the vehicle's unsprung mass; higher unsprung mass is harder for the suspension to control. Thirdly, the rim mass contributes to the vehicle's yaw inertia, an important factor impacting the cornering responsiveness of the car. Yaw inertia is calculated using the following relationship:

$$I = \sum md^2$$

The rims, which lie at the far extremities of the vehicle, are very influential in this calculation because the distance term is exponential. Therefore, reduction of rim mass is a particularly effective way to improve cornering response.

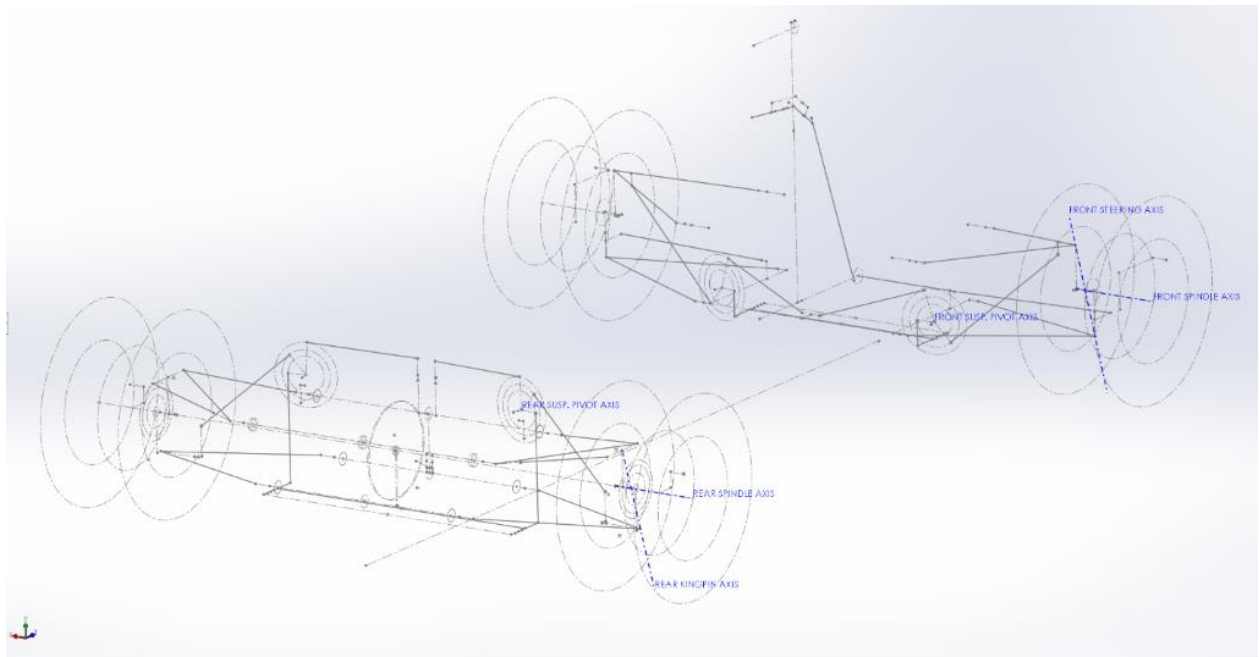


Figure 1: Suspension Geometry of GRC19

A major weight reduction would improve these characteristics, and also result in a significant reduction in total vehicle weight (on GRC18 the rims constitute around eight percent of the car's total curb weight). The use of smaller diameter wheels this season lowers the centre of gravity of the car; the centre of gravity of the rims and tires as well as all other unsprung components can be lowered by approximately 2.25 inches with the smaller 16" tires. This mass constitutes around 20 percent of the car, leading to a total CG reduction of around 0.4" in the vehicle.

### Impact of Stiffness on Vehicle Performance

As the part which transfers all forces between the car and the road, the high loading in the rims makes them a major source of suspension compliance. Other sources of compliance include the stiffnesses of the hubs, uprights, a-arms, and frame mounts, as well as free play in all connecting spherical joints, rod ends, and bolts. When designing a car, suspension compliance is to be minimized as it causes the tires to deviate from their intended orientation and range of motion, undermining the suspension's kinematic properties. One such example of this is positive wheel camber during roll. Positive camber is very detrimental to tire dynamics during cornering; it is often the case that designers set up their kinematics in a manner they believe will make this theoretically possible, yet have it occur once the car is built due to compliance.



*Figure 2: Example of Positive Camber in Cornering Due to Suspension Compliance*

Increased rim stiffness can help to reduce compliance in suspension, therefore making the system more predictable and controllable.

### **Summary**

Implementation of rims that are lighter or stiffer can result in major performance improvements to the FSAE car. At first glance, it appears that pursuing mass reduction during design will yield a greater overall improvement to the car. However, the most appropriate balance of strength and stiffness for the design will not be determined until structural analysis can provide further information.

## **1.2 BACKGROUND INFORMATION**

---

### **Load Case Determination**

In order to carry out the structural analysis, which will be used to choose the quantities and orientations of carbon laminae used, suitable loading cases to apply in the FEA simulations must first be determined. These simulations are to be done comparatively to the current aluminum wheels, with the success of the new design judged on the relative improvements it offers towards achieving the performance requirements.

To determine the loading cases, the most strenuous situations encountered by the wheels are investigated. Vehicle dynamics analysis is required to determine the maximum forces on a wheel in each of the coordinate directions, reflective of the different types of loads seen in driving situations. There must also be consideration for other stresses acting simultaneously due to tire pressure and inertial loading. The coordinate axes defining the forces on a rim are shown below in Figure 3.

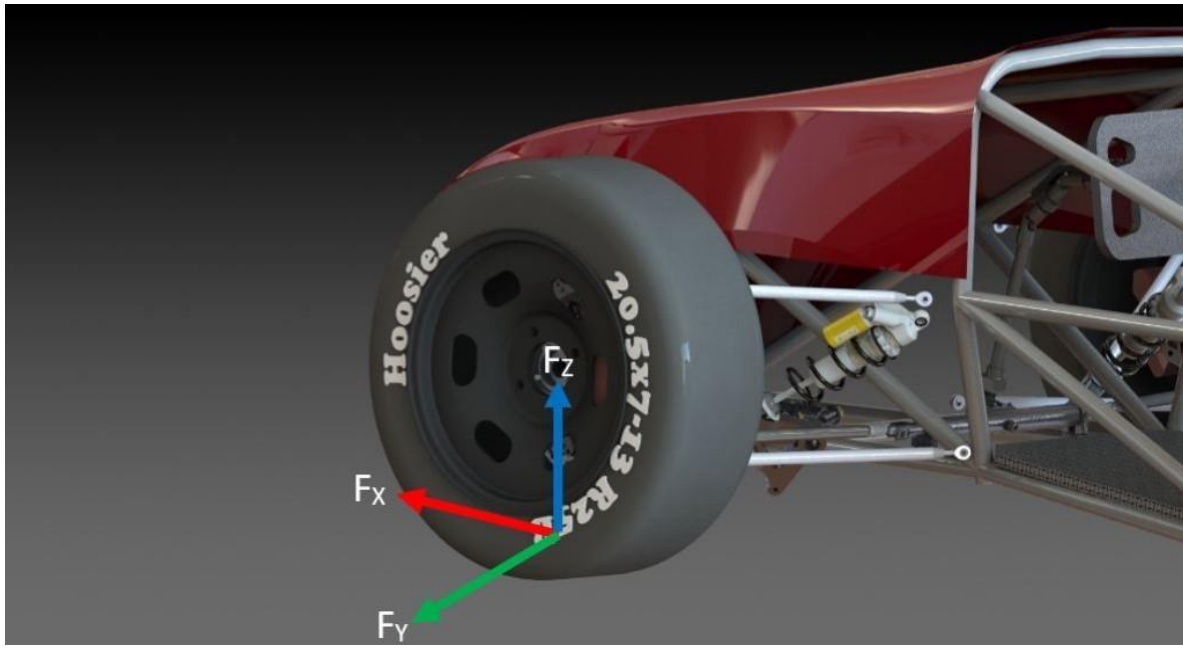


Figure 3: Standard Convention for Forces Acting on a Wheel

### Case 1: Maximum Longitudinal Force Conditions

This case is to be representative of straight-line acceleration and braking. Longitudinal forces (x-direction) are caused by the driving and braking torques. They put a torsional load on the rim about the centre axis of the spindle. This information is typically determined by tire test data, however there is no longitudinal data available for the tires being used as they were only recently released. A reasonable approximation can be made by examining the ratio of maximum longitudinal force to lateral force in the data of similar tires and multiplying the maximum lateral force, which is known, by this proportion.

$$F_{X(\text{Max.})} = 1.05F_{Y(\text{Max.})}$$

$$F_{X(\text{Max.})} = 1.05(2792.0\text{N})$$

$$F_{X(\text{Max.})} = 2903.7 \text{ N}$$

To be applied in conjunction for this load case are:

- Normal force ( $F_z$ ) of 1100N: This force represents a longitudinal weight transfer of approximately 80-20 %, which suspension analysis has found to be a reasonable expected amount for maximum longitudinal acceleration.
- Tire pressure force of 101 kPa (14 psi). This pressure represents the maximum upper range of pressure that could be expected for use in an FSAE tire. Note that the maximum longitudinal and lateral forces are taken at 10 psi however, because force is highest at this pressure. Although these are not capable of being true at the same time, this approach keeps the load case conservative.

- Inertial loading of 140 km/hr: This is the theoretical top speed experienced by the vehicle during a race.

### Case 2: Maximum Lateral Force Conditions

This case is to be representative of maximum lateral g's in a steady state turn. Lateral forces (y-direction) are caused by cornering and put a bending load on the rim. Shown below is a plot of lateral force on the selected tires vs. slip angle, a quantification of how the tire's line of travel deviates from its heading as a result of tire deformation. The plot used is for a value of 10 psi, the lower bound of possible operating pressures, as maximum lateral force is inversely proportional to pressure. The five colors correspond to different values of normal load. The curve of interest is in yellow, which represents 1100 N.

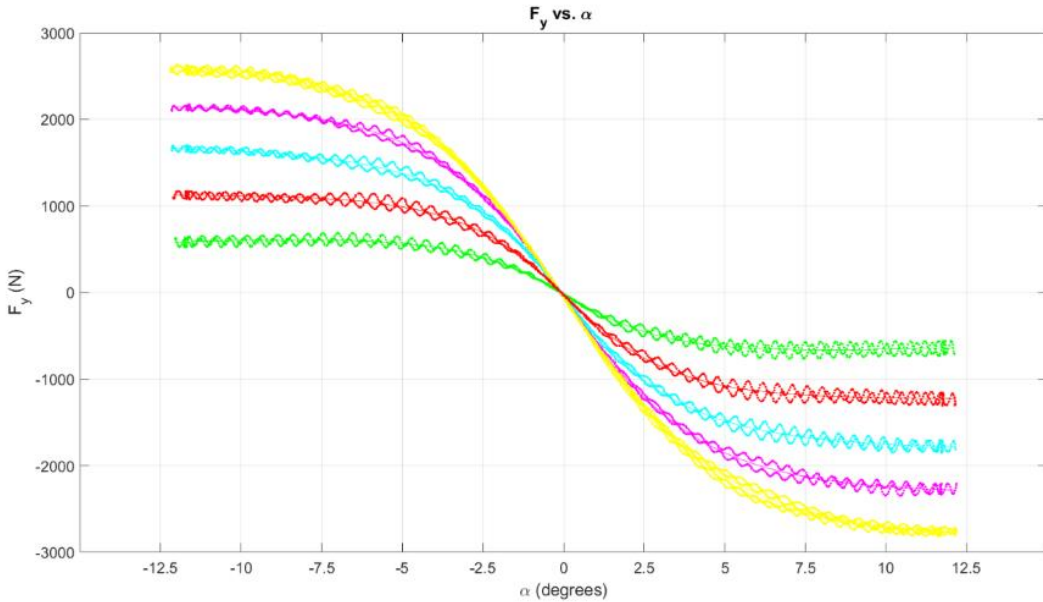


Figure 4: Normal Load due to Lateral Forces and Slip Angle (Tire Deformation) at 10psi

From the plot,

$$F_{Y(\text{Max.})} = 2792.0 \text{ N}$$

Again, 1100 N was selected as the value of normal force, using lateral weight transfer of around 80-20 % as a realistic upper estimate. The other forces to be applied in conjunction with this lateral force are:

- Normal force ( $F_z$ ) of 1100N.
- Tire pressure force of 101 kPa (14 psi).
- Inertial loading of 140 km/hr.

### Case 3: Maximum Normal Force Conditions

This case is to be representative of hitting a large pothole or bump. Although the car typically drives on quite smooth tracks, it is sensible to test this separately to ensure that the car can handle this situation. Normal forces (z-direction) are determined by the weight distribution in the vehicle at a given instant as well as bumps from road irregularities. This force puts a radial load on the tire. Because much of the tire's stiffness comes from the pressure of the air inside, a large proportion of these loads are transferred to the rim as a uniform compression on the entire outside face of the rim shell. The remainder of the force is transferred to the underside of the rim's tire bead surface through the tire sidewalls. The proportioning of how these loads are resolved between these two mechanisms is not known; the normal force is therefore assumed to act 100% through the sidewalls, as the other means (through air pressure) essentially causes a hydrostatic stress on the rim and is therefore a less severe load.

The maximum normal force was taken to be that applied during a 3g bump to one of the wheels. This is a realistic magnitude to represent a large pothole or bump.

Bump Condition			
Dim		Front	Rear
	Bump G's	3.0	Accel.
	Vertical Load (One Wheel Z)	2118.960	2295.540
		N	

Figure 5: Maximum Normal Force on One Wheel

The difference in front and rear forces is driven by the static weight distribution of the car. Maximum normal force is the higher number of the two:

$$F_{Z(\text{Max.})} = 2295.5 \text{ N}$$

The other forces applied in this case are:

- Tire pressure force of 101 kPa (14 psi).
- Inertial loading of 140 km/hr.

### Case 4: Maximum Inflation Pressure

The maximum possible inflation pressure is the last loading case that needs to be considered. No vehicle dynamics analysis is needed for this case, as the value of failure is determined using FEA. Maximum inflation pressure is relevant when mounting tires as the machine applies bursts of pressure to seat the tire bead onto the rim. A maximum psi rating should therefore be determined.

### Loading Case Limitations and Sources of Inaccuracy

Although the maximum force situations in each of the coordinate directions are an intuitive way of organizing the design approach, it should be kept in perspective that other force combinations on the tire are possible. Shown below is a traction circle for the selected tires written in Matlab. The ellipse represents the maximum limit of the tire's traction capacity at different proportions of longitudinal and lateral force. The ellipse is asymmetrical about the abscissa because more acceleration is available in

braking than from the two driven wheels. This figure illustrates that there are other combinations of longitudinal and lateral force along the curve which could potentially stress the rim more. However, this traction circle is only an idealized version, real traction circles are less uniformly shaped and require track test data which is not available.

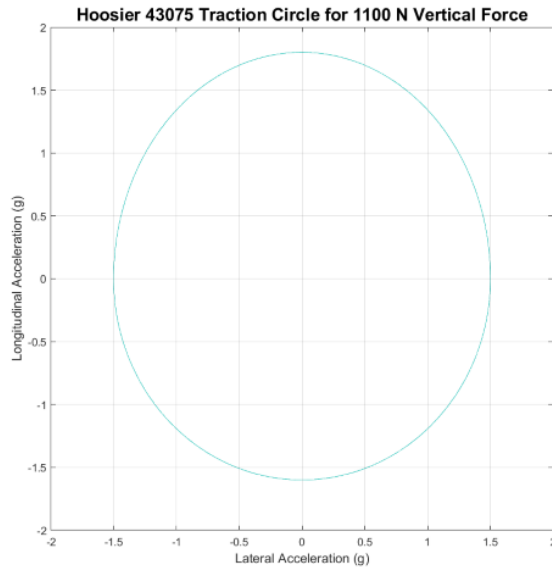


Figure 6: Traction Circle for 1100N Vertical Force

Another source of limitation is how the tire test data used was collected. All forces in the test are essentially “too perfect”, as they are done on a very uniform sandpaper-like test belt, with the tire within perfect operating temperatures. Tire test data is supposed to be adjusted with correction factors that are determined from driving test data, so that a more accurate model can be converged upon. This means that forces assumed for longitudinal and lateral force are likely conservative.

Upon implementation of a sufficiently sophisticated range of sensors in the Gryphon Racing vehicles, these loading cases should be revisited and further refined.

### Tire Heat Generation

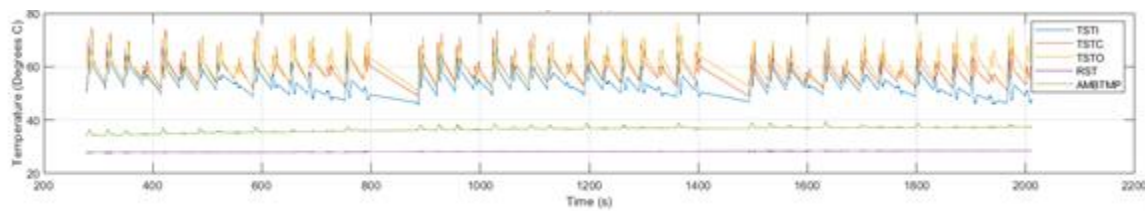


Figure 7: Tire Temperatures during Lateral Test

Heat generation from the tire tests is now observed to verify to what degree the tire will heat the rim. This is of interest because the epoxy used for carbon generally softens at excessive temperatures. Shown above is a plot of the tire temperatures recorded during the lateral test. It is seen

that tire tread temperatures reach a range of about 75 degrees Celsius at maximum. This amount of heat generated by the tires is not serious enough to cause issues with the epoxy selected. The epoxy is stated to be safe under temperatures of around 140 Celsius.

## 1.3 LITERATURE REVIEW

---

Deciding on materials and processes for high performance rim design is difficult and research into the current racing market is important before a final decision can be made.

Rims are a key component in decreasing a race car's unsprung mass (the mass of the car that is not supported by the suspension system). Decreasing this mass will improve vehicle acceleration and control [5]. For this reason, the materials chosen for these applications are the ones that can reduce weight most effectively.

In the current market there are three main options for lightweight rim manufacturing. These options are magnesium alloys, aluminum alloys, or composites such as carbon fibre [6]. Aluminum is the most common rim material for most applications. It has a good weight to stiffness ratio and corrosion resistance. It is also much easier to machine and less costly than other alternatives, making it a more easily accessible option for smaller racing teams.

Magnesium rims have had a long history with the racing community. Their stiffness is comparable to that of aluminum with a 50% lower density as it is the lightest of all the metals [3]. Unfortunately, pure magnesium rims used early on in racing were susceptible to both corrosion and fire elements [10]. When exposed to heat from a burning tire or even prolonged contact with the road, these rims would combust violently due to the reactive nature of this metal. These rims were also known to corrode quickly, leading to pitting and failure. These factors led to their unpopularity in the following years. Now as technology has improved, it has been found that alloying magnesium (particularly with Yttrium and rare earth elements) can create good fire resistance [12]. This leaves a rim that is very light and stiff without the unfortunate combustible side-effects.

The third main option for rim design is carbon fibre. Unlike the other two discussed earlier, this is a composite, in that it is composed of 2 distinct parts. The first is fibres of carbon, which give strength and act as the reinforcement. The second is a resin which permeates the sheets and creates cohesion, this combination is known as the matrix [9]. The result of this mixture is a material which is marginally lighter than magnesium alloys with much more stiffness (exhibiting a modulus of 228 GPa compared to 45 GPa for magnesium and 70 GPa for aluminum) and an ultimate tensile strength of 560MPa. These properties are ideal for modern racing rims, but they are also very expensive [4]. Machining CF is difficult as it can produce aerosolized particles which are known to be irritant and carcinogenic. It is also very abrasive, leading to rapid wear on machining tools [1]. For these reasons, it is difficult and very costly to find shops which are specialized enough to create high quality rims. Despite these drawbacks, carbon fibre is still the lightest material that can fill this role, making it the material of choice for high-end rims.

While CF has very good material properties for this application, it is an anisotropic material. This means that its properties are not uniform and will respond differently to loads in different directions. Within the material, individual carbon fibres are all oriented in particular directions (with some exceptions). For this reason, the material will be very strong when loaded along fibre lengths but will rely almost entirely on the strength of the resin when loaded perpendicular to fibres. The result of this in the context of rim design is that one must take the various load cases into account when deciding how to orient the various sheets of CF [9]. In this way it can be ensured that the material will be strong

enough in both the strong and weak axes. Unlike alloy rims, which will warp and stretch before they fail; CF will reach its failure point and fracture (brittle failure).

Once CF is selected as the material of choice, the next decision is the type of woven sheet that will be used. The simplest type of CF sheet is unidirectional. In this configuration, all the carbon filaments are oriented in the same direction. This is advantageous because this means that layers can be rotated in order to ensure a particular strength in each direction, to match the expected loading very specifically. Unidirectional is very flexible and can easily drape over complex geometries and contours.

The next CF configuration is known as a plain weave. It features a 1 by 1 weave of CF strips. Weave has equal strength against planes stress in two directions, making it more suited to applications where forces are relatively equal in each coordinate. This has been found to be the case during load case analysis of the rims. It also allows less severe rotation of the adjacent layers during layup which will lead to more uniform properties throughout this material. This variety of weave has the poorest drapability, due to the tendency of the 1x1 weave to hold itself tightly together.

The final CF sheet layout is a 2x2 twill weave. The double parallel strands reduce the strength of the final material slightly but make it far easier to drape around the complex geometry required to make a rim. The twill pattern increases strength and density, which will raise weight slightly, but keep the properties of the material within the target values [8]. The 2019 FSAE car makes use of 2x2 twill weave in other sections, and it has been selected for use in this project. This choice has been made because of the drapability, the relatively even loading in each direction, and the cost savings, as this material is already available to the group. Potentially, some sections of a CF rim could be reinforced with unidirectional CF, but performance gains would likely be marginal and this was too costly for the 2019 season.

Having chosen a weave type, the next decision one must make is between a wet layup or a prepreg autoclave procedure. Both of these involve CF sheets cut into the proper shapes for the application and epoxy, but they are very different in their implementation. Prepreg features sheets with a premixed epoxy solution applied to the carbon in a thin layer by a machine. These sheets are then laid up onto the mold and cured with constant temperature and pressure in an autoclave. In a wet layup, epoxy is mixed and layered onto dry carbon sheets manually, layer by layer. After this it is vacuum bagged and allowed to cure at room (or slightly elevated) temperatures. The difference between these two methods is in the precision with which variables are controlled. Manual layering generally has greater thickness and can be uneven or poorly mixed in places. For this reason, the true golden standard of composites is prepreg cured in an autoclave, where layers are far more likely to be uniform and imperfections are minimized.

Unfortunately, an autoclave is a very large, expensive, and energy-consuming machine to which access is often limited. A wet-layup will be available at a fraction of the cost and can be assembled using relatively inexpensive materials. By exercising extreme care in the mixing and application of the epoxy on the wet layup, one can achieve strengths and thicknesses very similar to the prepreg method [7]. After selecting a layup method, the final step in a CF process is epoxy and hardener selection. This combination of materials will be responsible for out of plane stresses and adhesion in a CF part and is therefore very important in achieving success. Although there are many different types of epoxies with various properties, there are 3 main things that must be kept in mind during selection. These are temperature resistance, strength, and cure-time. Temperature resistance is important because many epoxies will begin to lose hardness and fail at certain temperatures. To produce rims, tire heat data was found to have temperatures up to 75 degrees Celsius. This temperature must be withstood by whichever resin is chosen. Strength is a straightforward property for these purposes, it should match the necessary strengths for the various loading cases expected for the tire. The final factor for resin and hardener selection is hardening time. It is crucial that the layup does not harden before the vacuum

pressure has been established. This means that as the number of layers increases, a hardener with a longer hardening time must be selected to prevent inconsistent curing [2].

The current methods and materials for rim manufacturing are widely variable and there are many factors that must be taken into consideration. Each process must be tailored to the needs and particular goals of the process. By taking time to select optimal components, the best possible outcome can be achieved.

## 1.4 SCOPE AND OBJECTIVES

---

### Objectives:

- Determine realistic design load cases through vehicle dynamics analysis.
- Perform materials research to select appropriate fabric and epoxy types.
- Develop a carbon fibre rim design to meet the performance targets.
- Design and manufacture the required aluminum molds.
- Build a completed prototype rim.

The summarized objectives of the project are seen above. The project focused on the design and fabrication of carbon fibre rims. It began with tire and vehicle analysis to determine suitable loading criteria upon which to base a rim design. Force analyses using ANSYS to determine the stiffness of the previous aluminum rims were also completed. An ANSYS analysis of composite carbon fibre rims was performed in order to estimate the number and placement of layers of carbon fibre weave that would achieve a stiffness comparable to the aluminum rim. A custom rim profile has been developed for this new design, with consideration of suspension design criteria, ease of mold release, and minimization of stress concentrations. The final design iteration included 11 layers and approximately matched the stiffness of the original aluminum rims while minimizing the amount of carbon fibre used in order to reduce weight, all while maintaining a thickness of the rim less than 1/8". The performance targets set for the rim design follow below.

### Performance Targets

- **Strength:** Because of the possibility that the produced rims will not be as strong as predicted due to manufacturing imperfections or other sources of error, the rims were designed to have a higher factor of safety than the aluminum rim.
- **Durability:** The rims should have infinite expected life under fatigue analysis.
- **Stiffness:** Stiffness comparable to the original aluminum rims will be considered successful. Stiffness greater than the original aluminum rims while reducing weight would be preferred.
- **Weight:** A weight reduction of more than 10% (while maintaining comparable performance) would be successful, 25% or more would be considered very successful.

A full mold assembly has been designed, it is made up of four separate main sections and four smaller additional pieces which are added to the sides. The four main pieces that make up the mold were designed so that they could be fastened together accurately for layup, then easily disassembled to remove cured parts. To manufacture the mold, blocks of aluminum were first faced manually to the

required dimensions, and all required fastening features machined. Following this, the mold was machined using the Advanced Manufacturing Lab CNC mill to provide high accuracy machining of the rim profile.

Once the mold was completed, prototyping of the carbon fibre rim was carried out. Throughout the prototyping process, small test parts were made in order to practice the process of laying up and vacuum bagging carbon fibre. These test parts were also used in material testing to determine the actual physical properties of parts manufactured by the team. ANSYS models of the carbon fibre rims were verified using measurements of ultimate tensile strength, density, and layer thickness for the carbon fibre parts.

The layup process then followed, and a rim was manufactured by hand. A carbon fibre weave was laid onto the mold and using a vacuum bag to apply pressure, the laminated layers were set (this process is explained further in Section 2.3). The rim was then machined, and a clear coat was applied. This prototype was proof that a carbon fibre piece could successfully be created using the mold and layup technique.

The overall success of this project was measured by the progress towards establishing and documenting a reliable in-house process for manufacturing carbon fibre rims using the facilities and knowledge available to the Gryphon race team. The project team recognized that the production of a complete set of suitable racing rims is a lofty goal and will require the efforts of future students to complete the work. For this reason, attention was paid to documentation and reproducibility of manufacturing methods so that the project may continue and carbon fibre rims for a future Guelph racing team will still be produced. Therefore, the ultimate goal of this project has been to leave future students with the documentation, molds, and tools necessary so that the designs can be refined and carbon fibre rims can be regularly manufactured for the Gryphon race team.

## 1.5 CONSTRAINTS AND CRITERIA

---

The various restrictions which will play a role in developing a suitable rim and mold design are outlined below. The manner in which these factors limit and influence design decisions will be further discussed throughout the design explanations as relevant.

### Constraints

- Reduce the weight of the rim by at least 10% (preferably 25%).
- The rim profile must have suitable geometry such that the tire can be mounted.
- The mold must be physically possible to machine. There cannot be any negative angles to mill, and milling cannot be done deeper than the length of the available tooling.
- The mold must be able to facilitate mold release by some means.
- Geometry of the rim shells cannot be such that they are mechanically locked into the mold after layup.
- The width of the rim must fall within the specified acceptable range (5.5-7.0") for the selected tires.
- The rim offset must fall within the range of +10 to +30 mm as dictated by vehicle suspension design requirements.

- The rim must use a 12-hole bolt circle of diameter 6.75 inches, with each hole of  $\frac{1}{4}$  inch diameter, for the mounting of the available rim centres.
- The rim must be entirely airtight up to a value of 100 psi.
- There must be some means of tire inflation/deflation incorporated into the rim.
- The rim must be designed such that the tire will not de-bead during operation.
- Inside diameter of the inner rim section must be equal to or greater than 9.35" to accommodate suspension packaging requirements.
- Any machining, sanding, polishing, or other post-processing of the carbon rims must be performed with air extraction available to reduce the risk of adverse health effects which are associated with carbon fibre dust.

#### **Criteria**

- All mentioned performance targets should be satisfied.
- The carbon weave used should have as high drapability properties as possible to facilitate proper layup on complex surfaces.
- The directions of the carbon lamina should be oriented proportionately to the applied loads.
- Any machining, sanding, polishing, or other post-processing of the carbon rims should be minimized to reduce the risk of adverse health effects which are associated with carbon fibre dust.
- The molds should be made from material that is available to the group at minimal cost.
- The molds should be designed such that critical tolerances for the rim geometry (critical dimensions and surface finishes) are followed as closely as possible.
- The molds should be designed such that the cutting depth required for milling operations is kept within reasonable limits. Chattering can be encountered when using long tools at high speed.

## **1.6 PROJECT MANAGEMENT**

---

#### **Budget**

The budget of the project was constrained to the funding received through LabFund. Careful planning had to be conducted to ensure any additional costs could be kept to a minimum. For example, the team initially considered the use of a third party to water cut the plates for the mold. By taking advantage of the CNC in the Advanced Manufacturing Lab, this cost was avoided. The team also initially believed that a new vacuum pump would have to be purchased as the one available would overheat and leak oil. By repairing the old one, this cost was also mitigated. Mold constraints led to a significantly increased number of fasteners, but this had a relatively small impact on the budget of the project.

#### **Schedule**

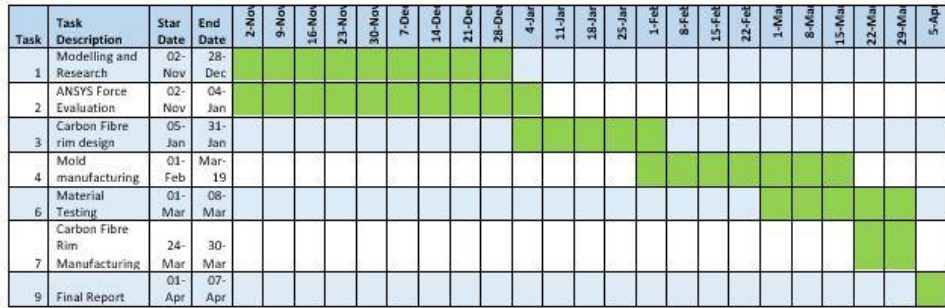


Figure 8: Updated Gantt Chart

An updated Gantt chart detailing the team's schedule is shown above. Every task necessary for the completion of this project has been performed. Modelling and research took place for two months to make sure all information needed to pursue this project was acquired. FEA using ANSYS also took two months as the team had to wait for CAD of the aluminum rims to arrive before any analysis could take place. Rim design only took one month as very few changes had to be made to the CAD of the aluminum rims in order to create the carbon fibre ones. Some changes included a draft angle added to the larger half of the rim and a curve that was added to the smaller half. Mold manufacturing occurred after a rim design had been finalized. For a month and a half, the team created and revised their design for the rim to ensure the best product would come from their work. Material testing also took place during this time to confirm that the carbon fibre rim would be stronger and lighter than the aluminum one. After testing took place, the rim was finally created. The last task for the team was the final report, which the team allotted one week for.

The resources required for this project included: tools and space to work safely with carbon fibre, access to large amounts of time in the machine shop, and the acquisition of the raw materials purchased with the lab fund. The tools needed to work with carbon fibre were borrowed from the race team. Cutting carbon fibre results in the release of potentially hazardous particles into the air, which is dangerous when breathed into the lungs. The race team shop was the best option for the team, but it was decided that in order to use this shop, an extraction system would be needed to dispose of the airborne carbon fibre filaments.

Some challenges that were anticipated were related to the molding of carbon fibre parts. Working with carbon fibre was difficult and there were several potential errors that could have compromised the quality (and therefore the performance) of the rims or even the molds themselves. Poor installation could have led to poor appearance, performance of the rims, or the inability to separate part from mold, which would mean the destruction of all physical products of this project. In order to minimize these risks and familiarize group members with the intricacies of composite molding, several test parts had been created. Using knowledge gained from these trials, more test pieces were made with specific attention on the maintenance of complex geometry.

Several challenges were encountered and had to be overcome in order to progress in this project. One such issue was the early misconception that the provided aluminum plates were large enough to accommodate the rim geometry. While this proved to be false, some modifications to the mold quickly solved this issue. Another problem discovered was the rigidity of the carbon fibre sheets that were in the FSAE shop. During testing, the team discovered that sheets of this rigidity would not be

able to cover the particular geometry of a rim. Far more flexible weave was found, which were more difficult to cut cleanly, but easily formed to the curves of the design. Some of the early test pieces had proven to be unsuccessful, but the team was able to form a hard hat with a fair degree of strength and dimensional accuracy. Before an attempt to make rims was made, the team continued to learn as much as possible about the carbon fibre manufacturing process through trial and error with simpler geometries. This way, many problems that related to material properties were solved so that the team could focus efforts on meeting geometry related difficulties when the rim layup stage of production began.

## 2.0 DESIGN METHODOLOGY

### 2.1 RIM DESIGN

---

#### Material Selection

The 2x2 twill weave carbon fibre available in the FSAE race shop is the primary material used to make the rims, due to its ability to easily distort and drape around the rim geometry during the layup process. Using material that is already available also allows the cost of the project to be minimized. The epoxy chosen is Aeropoxy PR 2032 resin which is often used in high performance structural applications of composites. Because the rims are not merely an aesthetic part and will be experiencing strenuous loading during use, a strong epoxy must be used. The hardener paired with this epoxy is Aeropoxy PH 3663, which is a common hardener for fabricating carbon fibre parts and has an intermediate working time of 90 minutes. This provides ample time to successfully run through an entire layup process. The peel ply chosen for this project is Airtech Bleederlease B peel ply. This material is infused with silicon to ensure efficient release from the composite and epoxy. The cotton, vacuum bagging, and other intermediate plastic layers used in the layup process were also found in the FSAE race shop, allowing further reduction of costs.

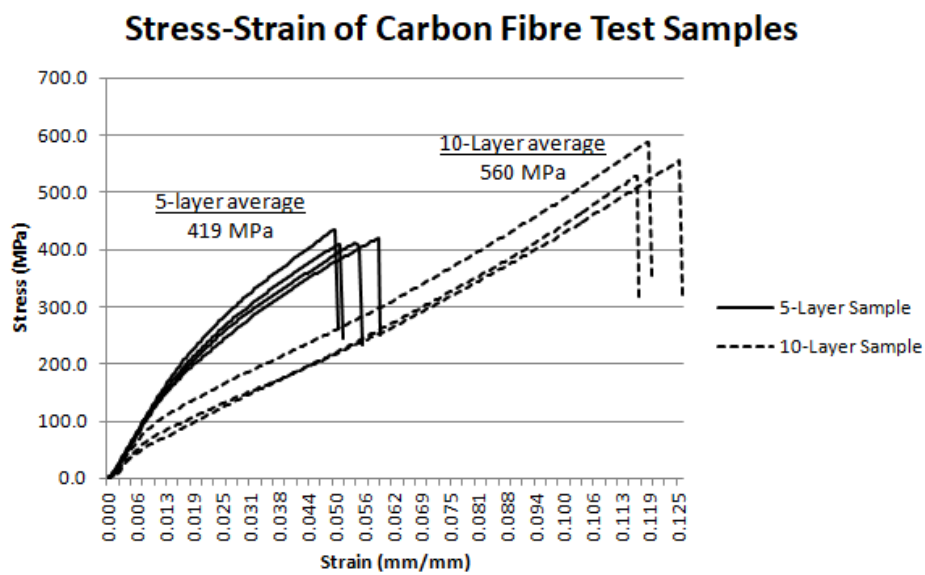


Figure 9: Resulting Stress Strain Curves from Ultimate Tensile Strength Tests on 5- and 10-layer Carbon Fibre Samples

In order to confirm that these materials met the requirements for this project, destructive testing was done on several samples. These tests were done on the universal testing machine (Instron) in the university of Guelph materials testing lab. This machine has a 100 kN capacity and is used to perform ultimate tensile tests. By performing this testing, a designer can ensure that the material properties used for analysis will most closely match the actual materials used. For this reason, all test sample strips were created using the same epoxy, carbon fibre, and layup methods that would be used in the final product.



Figure 10: Machined ASTM 370 Tensile Test Sample

For many materials, ductile failure occurs, producing a stress strain curve with 3 main sections. The first is the elastic region, a linear portion at the beginning of deformation from which the material would return to original dimensions if released. After this the material begins to deform plastically, meaning that it would be permanently deformed but unbroken if released. This section generally shows a stress continuing to increase with a decreasing slope. Finally, the stress reaches the yield point, after which it will decrease until the part fails.

As expected, the results for this test on the carbon fibre indicate a much more brittle material in that almost all deformation is in the elastic region, followed by yield and immediate failure. This is because carbon fibre is incredibly stiff and will deform very little before failure. The high modulus.

Looking at Figure 9, one can see that the yield stress on the 5-layer test strips is lower than the yield strength of the 10-layer strips. This is strange as stress varies with cross sectional area where failure occurred and should therefore be the same regardless of test sample size. This inconsistency is likely due to the human error involved in a wet layup. As stated earlier, there are many factors in a wet layup that could affect the final strength of the product. These include air bubbles in the resin, inconsistent resin layer thickness, and carbon fibre orientation. As there are a smaller total number of layers in the smaller test samples, any error in layup would have a magnified effect on the overall strength.

Despite minor inconsistencies, the average result of this testing was very close to the suggested values for carbon fibre. By performing this test, an accurate value of 560MPa could be used for all further FEA analysis of this design. Another benefit of this value is that it shows planned team layup procedure would be capable of creating high-quality carbon fibre parts.

With a strong baseline of material information, a design can be made that will realistically satisfy both strength and geometric criteria.

## Rim Geometry

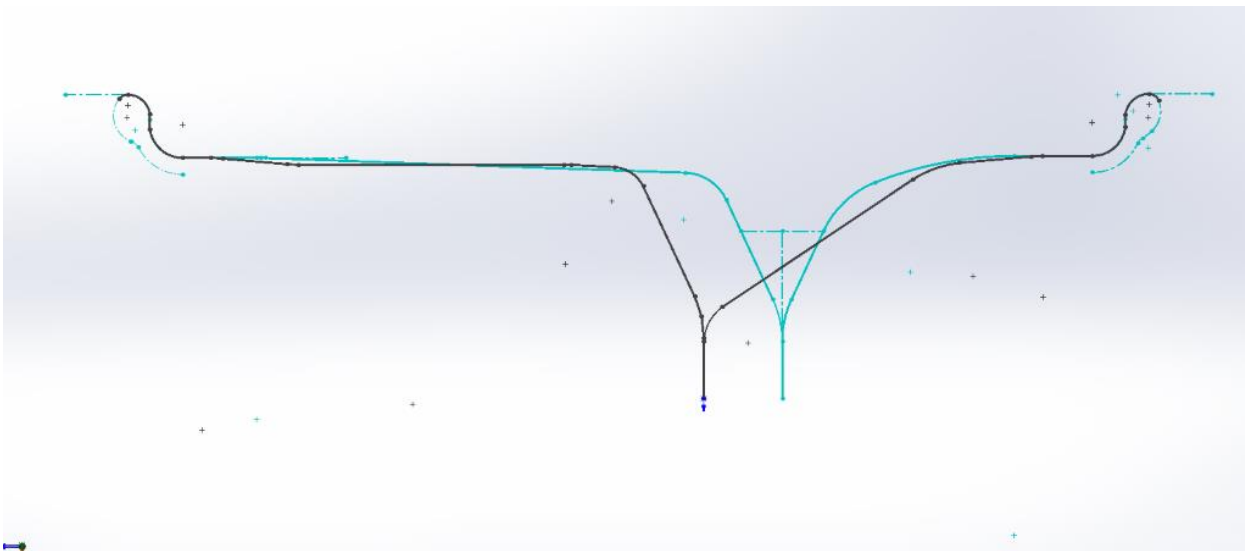


Figure 11: Comparison of Finalized Rim Profile (Blue) vs. Aluminum Original (Gray)

Seen above is a sketch of the finalized carbon rim profile overlaid with the original profile of the aluminum rim (Individual sketches available in Appendix Figures 29 & 30). The inner rim shell is seen on the left, and the outer shell on the right.

The revised rim incorporates a 2-degree draft angle into the inside rim section to facilitate mold release. 0-degree angles are not desirable because this places the part entirely in shear, in which the mold-part interface is strongest. An angle of only 2 degrees is used because of the limitations imposed on minimum rim diameter by suspension design requirements in that section. The revised rim features an increase in rim offset as well, from 12.7 mm to 27.7 mm. This decision was also made for suspension design considerations; the manufactured rims are made available in offsets of discrete 1-inch increments, however a value between two of these was determined as most desirable. This has the beneficial side effect of decreasing the mold's thickness in the outer rim's section, decreasing the depth of milling required in the thickest section. The sections where the rim profile curves out from the centre mounting surface has also been made the same for each section, and the adjacent curvature in the outer shell has been smoothed out. Because this design is not restricted to using a limited number of discrete radius tools like the spun-forged aluminum parts, this revised profile can reduce the stress concentration in this region.

The rims share the same tire bead geometry. For some rim designs, an additional "hump" is added inward of the tire bead area as an added means of keeping the tire securely seated during operation. In the absence of this feature, the tire bead relies on the friction at the tire-rim interface in combination with the outward air pressure to keep it properly seated. It would not be possible to add a feature like this into the mold because it would not be feasible to machine with a 3-axis vertical mill and it would also result in the rim being mechanically locked into the mold after layup. Extra thin strips of carbon could in theory be added on after the main layup process, when the part has been removed from the mold. However, this feature is not commonly used so it is assumed to be unnecessary to keep the

tire properly seated. In the future, if issues are encountered with tire de-beading, this idea will be revisited as modifications of this nature can be easily made.

## Structural Analysis

A model of the 10" aluminum rims selected for the 2019 season was downloaded from the supplier and uploaded into ANSYS for finite element analysis. Four loading cases were considered: max lateral force (cornering), max longitudinal force (accelerating/braking), max normal force (bump/pothole impacts), and max pressure (relevant for tire mounting). The rim and wheel assembly are considered as fixed at the hub mounting surface, with ground reaction loads applied as a remote force at the geometric centre of the contact patch. This analysis produced estimates of the locations of deflections on the rim and their magnitudes and it can be seen later in this report in figures 15 and 16. The deflections in each case were then the benchmarks when designing the carbon fibre rim.

After the design of the mold and the profile of the carbon fibre rim was finalized, further finite element analysis was conducted using the ANSYS composites package (ACP-pre) to model a carbon fibre rim. Tensile testing with 5-layer and 10-layer tensile test samples indicated a UTS of 450-560 MPa in X and Y. In the ANSYS project section "Engineering Data" the properties of CF layers were modified with the 560 MPa value found in testing. A shell of the mold geometry was uploaded to ANSYS and the rim was separated into an inner and outer hemisphere that were modelled separately and joined later for the structural analysis. The faces that carbon mats would be laid-up onto were added to "named selections"; these locations included two rings to reinforce where the profile of the rim changes quickly and at the tire bead. The number of layers, the location of reinforcements, and the orientation of the layers were changed iteratively, while comparing the resulting stiffness and strength of the CF rim to the aluminum rim.

It was found that the stiffness of the CF rim was greatly improved with strategic placement of areas of reinforcement where stress is concentrated (see Figures 12 and 13 below). Overlapping areas of carbon fibre are also inherent to the design since the curved geometry of the part can only be achieved by sectioning each layer into multiple carbon pieces, and these naturally must overlap in order to achieve 100% coverage of the curved faces in the mold. The tire bead area is reinforced as this section will be trimmed after molding and therefore is particularly vulnerable to fraying.

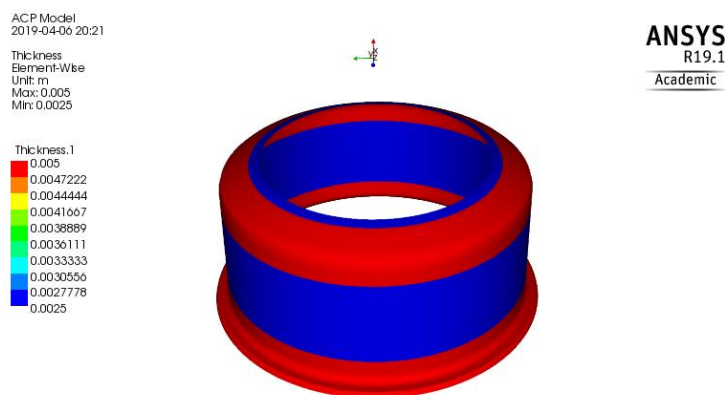


Figure 12: Thickness (m) of Inner Shell with 10 layers and 10 Reinforcing Layers (Red Areas)

ACP Model  
2019-04-06 20:26

Thickness  
Element-Wise  
Unit: m  
Max: 0.005  
Min: 0.0025

ANSYS

R19.1

Academic

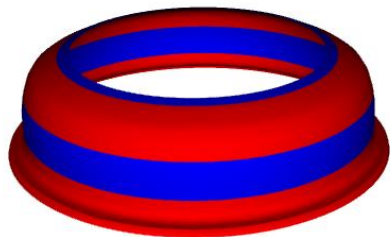
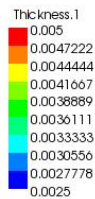


Figure 13: Thickness (m) of Outer Shell with 10 layers and 10 Reinforcing Layers (Red Areas)

The loads and fixtures that were used for ANSYS simulation are shown below in Figure 14. In Figures 15 and 16, the performance of a 10-layer CF rim with the layup outlined above is compared to that of the original aluminum rim. The 10-layer CF rim has a higher factor of safety in each case than the aluminum rim. The new design geometry lengthens the flattened barrel region and adds a draft angle. An unanticipated consequence of this is lengthening the moment arm of forces applied at the tire bead, which results in increased deformation at the inner shell's tire bead. The increased deflection is small, less than 0.6mm in the most extreme case.

The mass of a 10-layer rim is estimated at 1.18kg, which is  $10/6 \times 0.710\text{kg}$  (the mass of the prototype 6-layer CF rim).

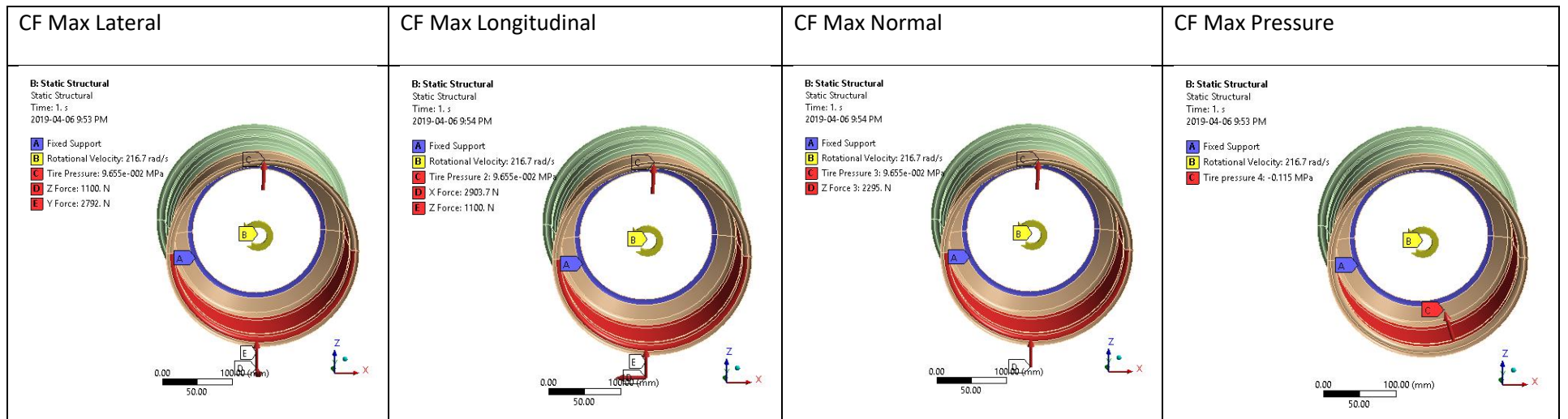
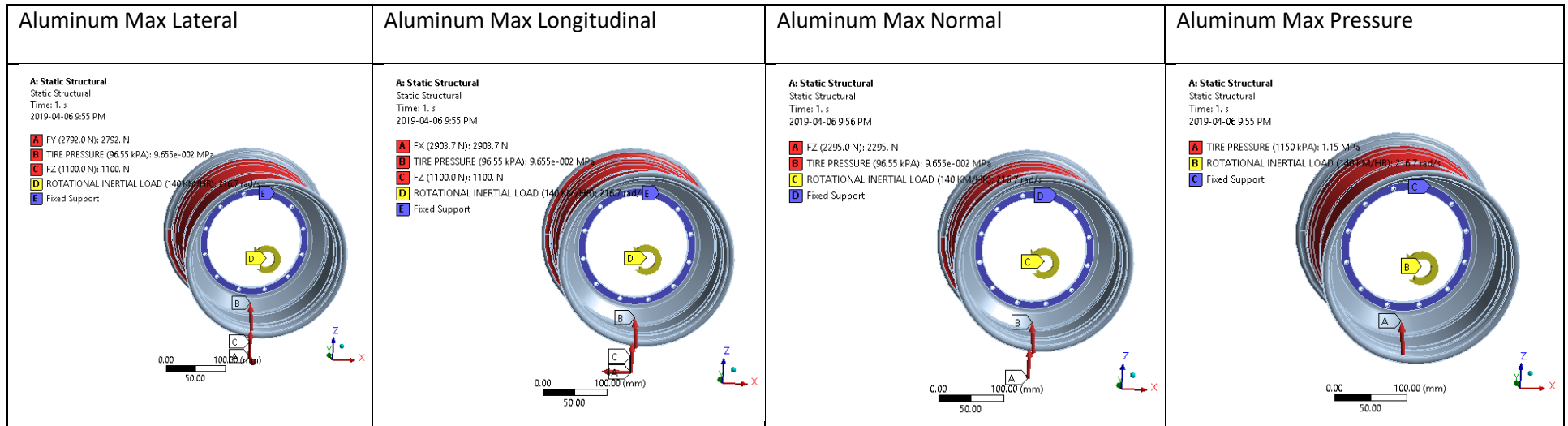


Figure 14: Loads and Fixtures. The above two sets of images show the location and magnitude of the applied forces and the chosen fixture points when ANSYS simulations were performed. From left to right, the cases correspond to: maximum lateral force, maximum longitudinal force, maximum normal or bump force, and maximum pressure. The first row of images represents the cases applied to the aluminum rim and the second row is the CF rim. In each case, the rims were subject to the same forces in the same locations.

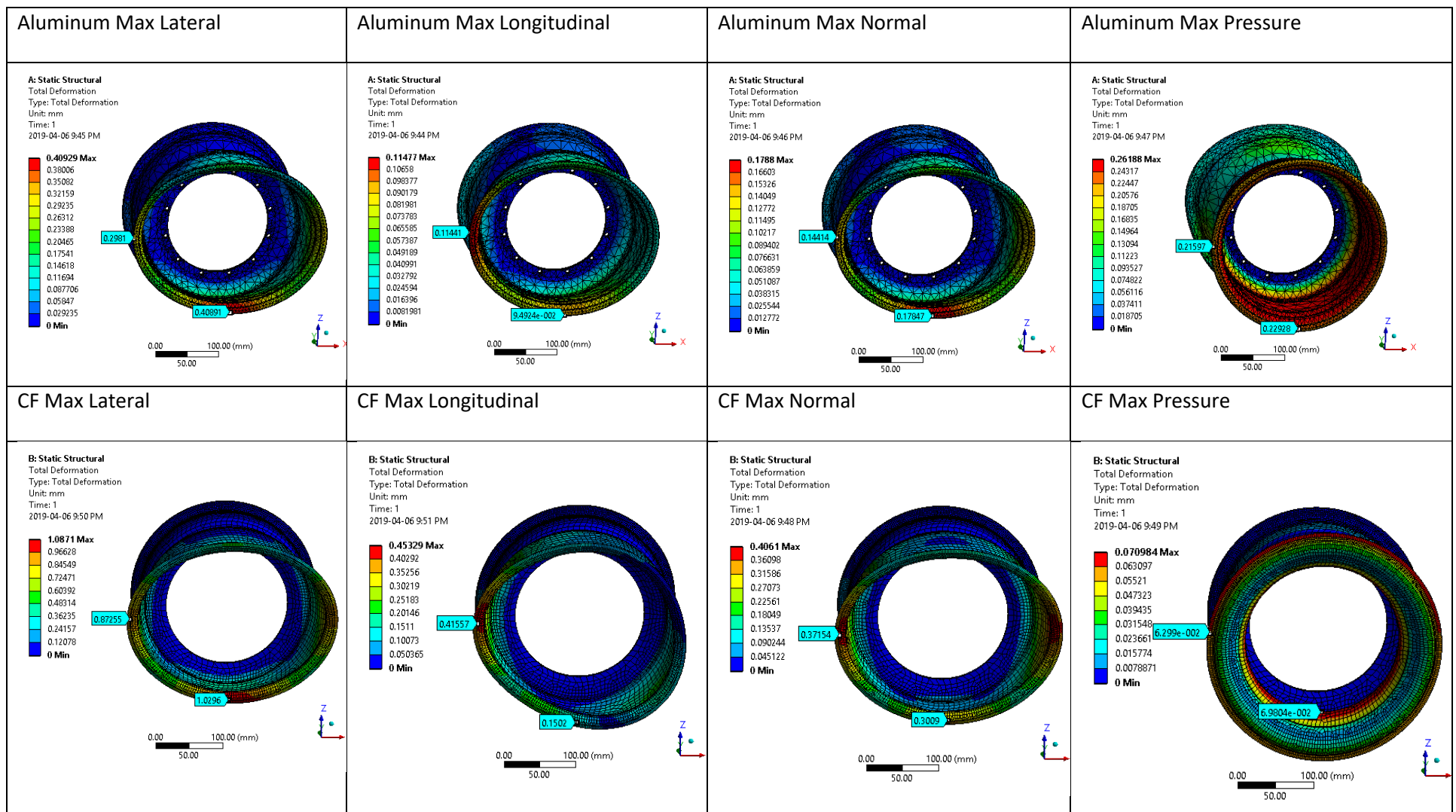


Figure 15: Deformation Comparison. The above two sets of images show the location and magnitude of deflections for the aluminum and CF rim when ANSYS simulations were performed. From left to right, the cases correspond to: maximum lateral force, maximum longitudinal force, maximum normal or bump force, and maximum pressure. The first row of images represents the cases applied to the aluminum rim and the second row is the CF rim. In each case the rims were subject to the same forces in the same locations.

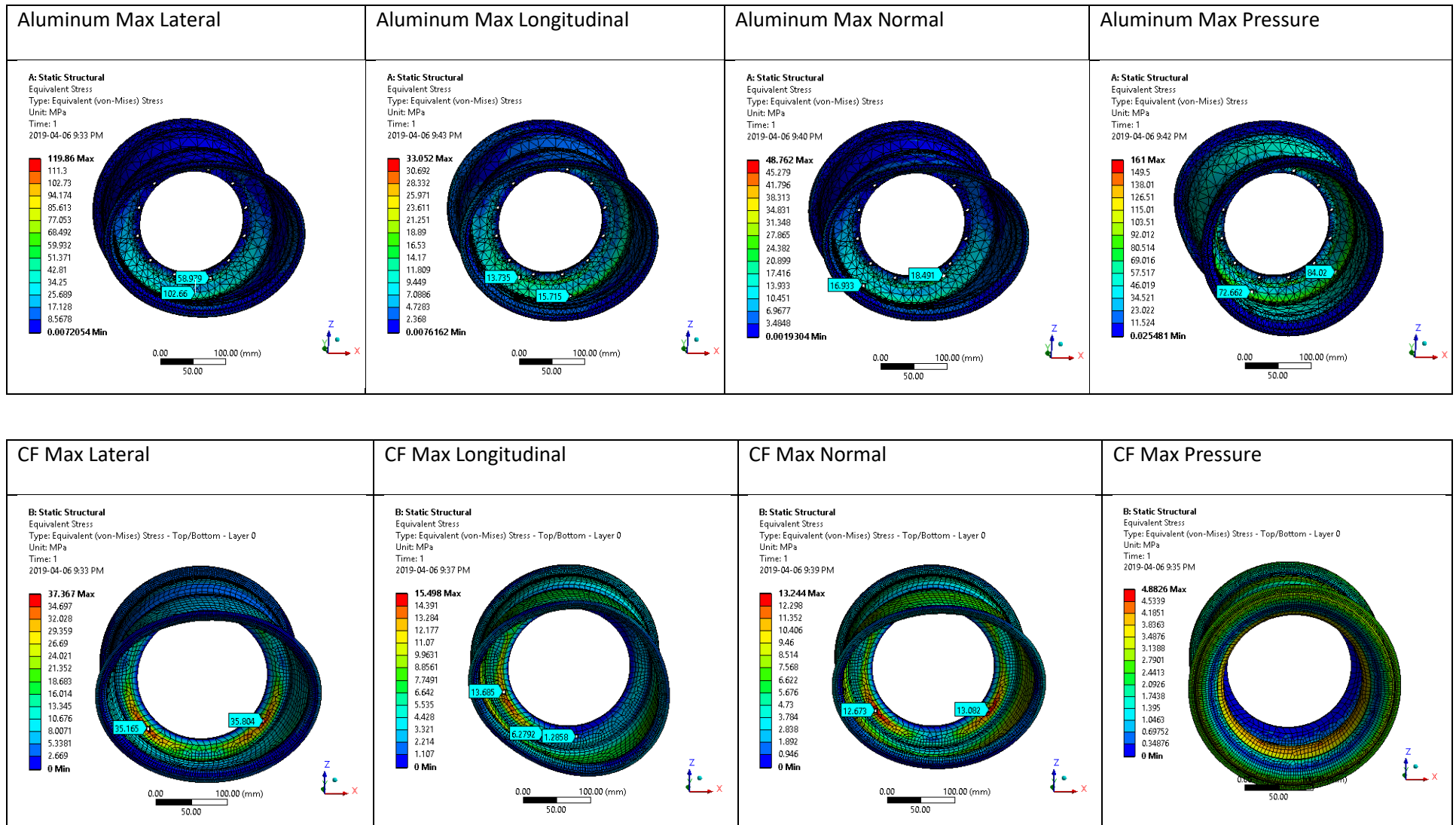


Figure 16: Stress Comparison. The above two sets of images show the location and magnitude of the applied stresses when ANSYS simulations were performed. From left to right, the cases correspond to: maximum lateral force, maximum longitudinal force, maximum normal or bump force, and maximum pressure. The first row of images represents the cases applied to the aluminum rims and the second row is the CF rim. In each case the rims were subject to the same forces in the same locations.

Based on the stiffness and mass of the prototype rim produced, as well as the above ANSYS simulations and the results of tensile testing, the following sensitivity analysis was performed in order to determine the optimum number of layers for an FSAE CF rim. The sensitivity analysis favours keeping the weight of the rim below 1.42 kg which is the weight of the aluminum rim. The term related to deflection percentage is squared to weight it heavily against rims that are low stiffness. The factor of safety term is weighted less than the other two terms as it is high even with few layers. With this weighting the optimum number of layers is shown to be 10 or 11 layers. With 12 layers the rim's mass would be nearly the same as the aluminum rim without an improvement to stiffness, though the factor of safety would be improved.

*Table 1: Sensitivity analysis was performed with the following equation:  $(1.42 - \text{Mass}) \times 30 - (\text{Def \%})^2 / 300 + \text{FOS} / 1.8$ . With this weighting the optimum number of CF layers is 11.*

CF Layers	Mass (kg)	Deflection (%)	Factor of Safety	Sensitivity Analysis
5	0.59	87.5	0.5	-0.39
6	0.71	80	1	0.52
7	0.83	72.5	3.25	2.03
8	0.95	65	5.5	3.17
9	1.07	57.5	7.75	3.93
10	1.18	50	10	4.32
11	1.30	42.5	12.25	4.33
12	1.42	35	14.5	3.97
13	1.54	27.5	16.75	3.23
14	1.66	20	19	2.12
15	1.78	12.5	21.25	0.63

## 2.2 MOLD DESIGN

---

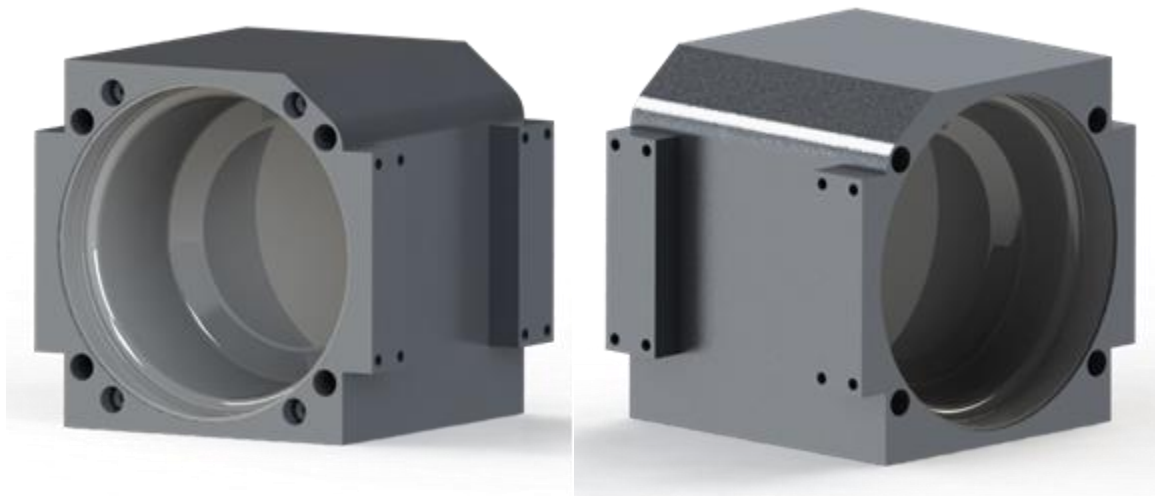


*Figure 17: Isometric Views of Final Mold Design*

## Type of Mold

A major decision to be made is whether to use an internal or external mold for the rims. A male mold would be made on a lathe or mill and would use the least amount of stock material. It also allows the possibility of mounting the assembly on a spindle to be rotated during the layup process. A female mold would require more material and would be made in a mill. It would require more vacuum bagging as the material must curve around and into the cavity.

A key consideration in this decision is which surfaces of the rim geometry are most important. The surface lain up on will be perfectly accurate to the mold and have superior surface finish. From this perspective, a female mold has a noticeable advantage. The tire bead geometry is of critical importance as there are tightly defined requirements for the rim-tire interface. Additionally, the rest of the outer rim surface must have a smooth surface finish so that seating the tires will be feasible. Lastly, the surfaces where the inner and outer shells attach to each other (the rim centre mounting feature) should be as smooth and flat as possible; this surface would also be covered with a female mold.

For these reasons, a female mold is best suited to meet the design requirements. The mold will be created out of 4.5" 6061-T6 aluminum slabs that are available to the group through the Gryphon Racing team. Aluminum is an ideal material for this detailed section due to its machinability. Also, as a high-density material, aluminum does not require any gel coat on the mold surface.

## Sectioning

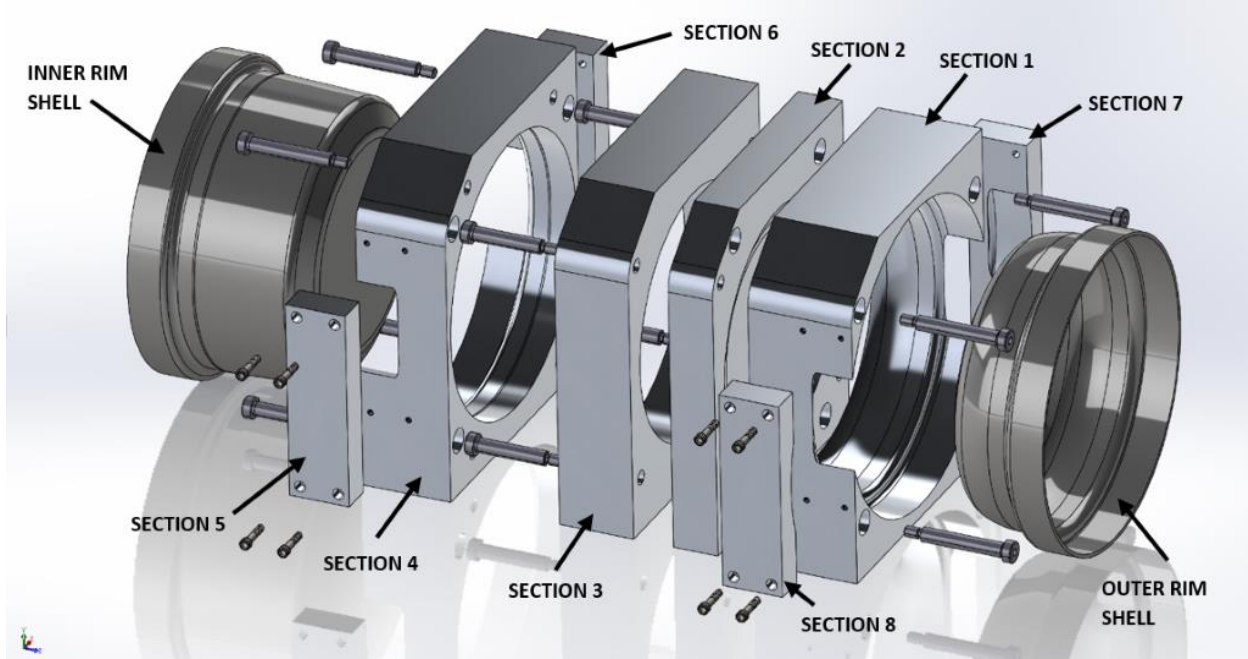


Figure 18: Exploded Final Mold Design

The mold consists of 8 aluminum blocks in total, with four major sections. The outer rim shell geometry is contained within Sections 1, 2, 7, and 8. The inner rim geometry is contained within sections 2, 3, 4, 5, and 6. Sections 5-8 are small blocks added on to the edge of the inner and outer rims because the available material is slightly too small to incorporate the geometry entirely. The major sections are

also rounded in one of the corners because of the shape of the available material (Appendix Figure 37). Note that only one rim shell will be created at a time, working exclusively with an assembly of their associated blocks. The designs are only shown as a full assembly as a convenient means of displaying all parts to be used. This would also be a convenient configuration for storage.

Section 2 is designed to be reversible so that it may be used for both laying up and drilling for either of the two rim shells. The sides used for laying up and drilling will be kept consistent such that one side is marked up from being used for all machining operations whereas the other is always used for layup and remains clean.

The edges of both the inner and outer rim shell geometry feature a continuation of the mold at the tire bead diameter. For carbon layup, it is good practice to create a bigger part than required because the edges often have issues with fraying and not saturating entirely. An additional 35 mm of length is provided so that this material may be trimmed away as excess.

With the goal of minimizing the number of sections required, mold development began from a version using three major sections (Appendix Figure 31). However, it was decided that it would be better to use four so that three of the sections would feature a “through hole” which could be waterjet cut out to expedite material removal and the fourth section would allow for the previously mentioned functionality of Section 2. Although it was decided that waterjet cutting would not be necessary, this through hole is still incorporated in the design to facilitate the layup process. The design was then changed to include a fourth section as a flat plate to incorporate these considerations. As the details of this configuration were further evaluated, concerns arose with this design as well. The flat plate connected with Section 1 caused a knife edge geometry in that section. This is not desirable because this feature could break, would be very sharp, and may not machine accurately. Also, in Section 1, the thickness of the part was very close to the upper limit of what depth can be machined. To resolve these issues, it was determined that it would be more appropriate to place the seams on either side of Section 2 as slightly inward on the rim curvatures rather than at their mounting surfaces. A cross sectional view of the final sectioning layout is shown below.

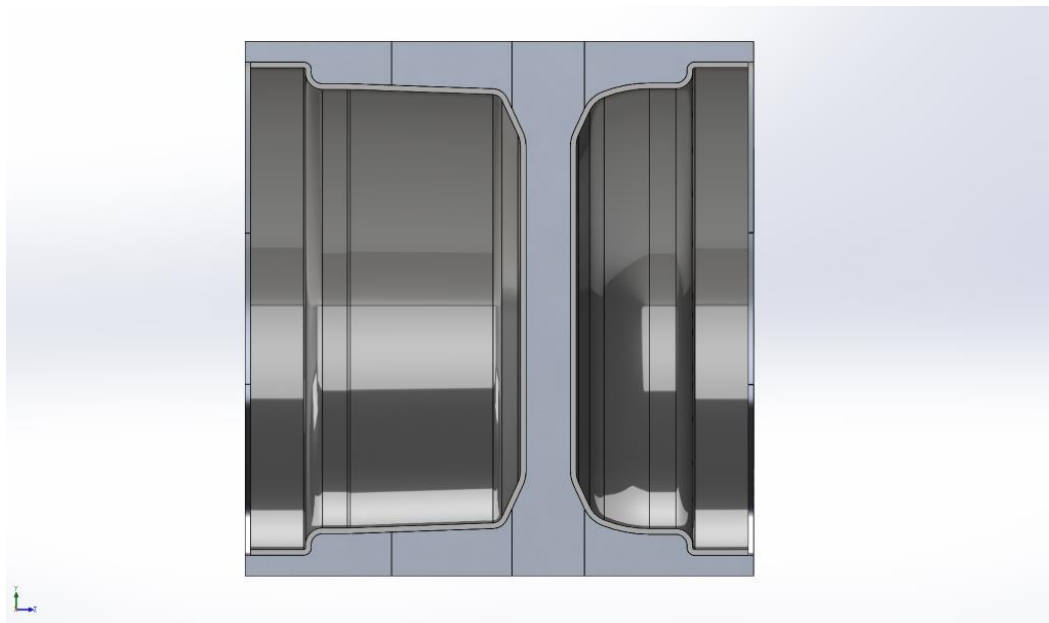


Figure 19: Mold Assembly Cross Section

## Fastening and Mold Release

The sections are attached and detached using a combination of socket head shoulder bolts and standard socket head bolts. Shoulder bolts are desirable because they allow the part to be both properly located and attached with one piece of hardware. A previous design consideration was to use standard bolts in combination with dowel pins to ensure proper location, however this adds additional room for error in the manufacturing process as it requires each section to be flipped (Appendix Figures 33-34). Using shoulder bolts allows the same functionality to be accomplished with less complexity.

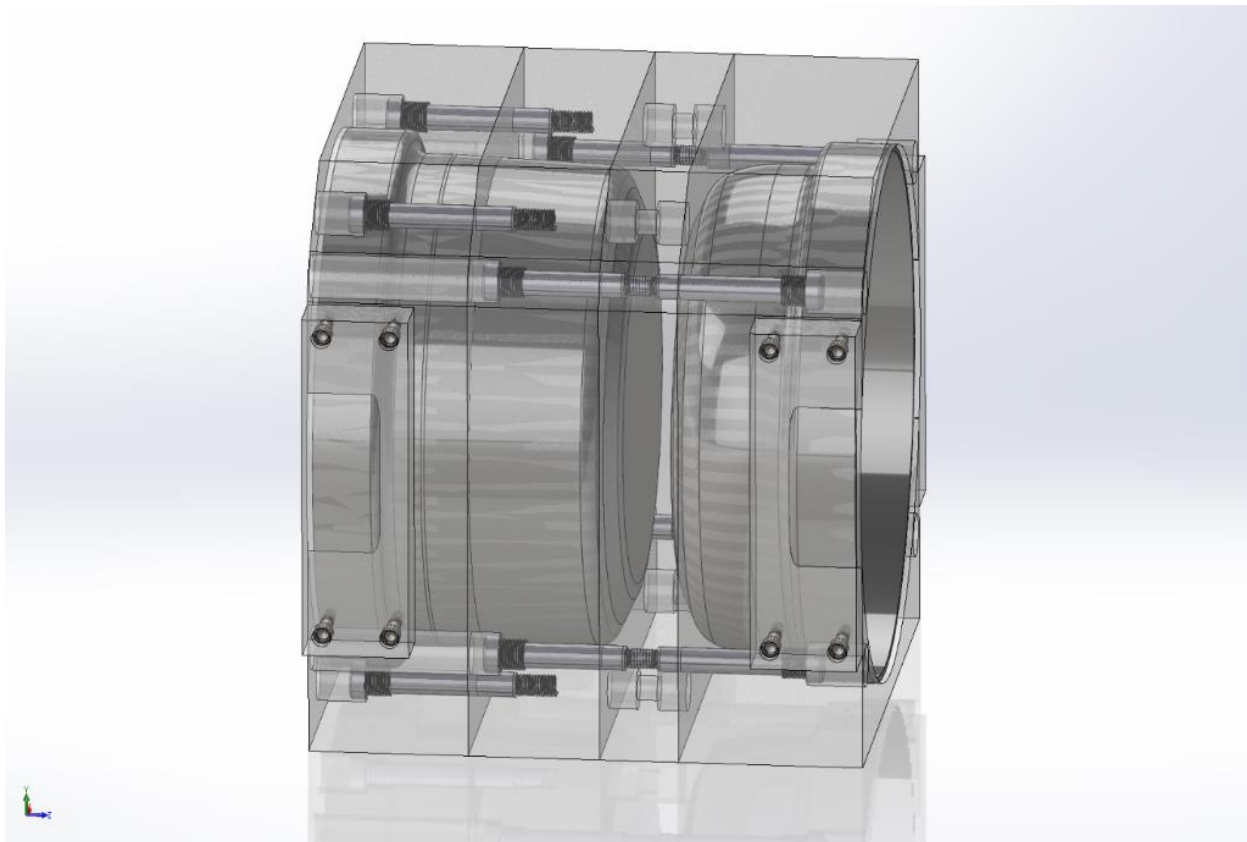


Figure 20: Mold Assembly Isometric View (Displayed Translucent for Detail)

Mold release is accomplished by separating the major sections and pressing the finished rim out using a hydraulic press (Appendix Figure 35). For the inner rim shell, this will mean removing Section 2, then Section 3, afterwards pressing the part out of Section 4 from above. For the outer rim shell, Section 2 will be removed before pressing the part out of Section 1.

The preliminary design explored the option of machining slit features between each of the major sections, such that wedge-shaped objects could be driven in to separate the parts (Appendix Figure 36). However, because the rims have a large amount of surface area and may require significant force to remove, even with proper application of PVA mold release, the team was unsure of the effectiveness of this method. An alternate strategy was developed; bolts were to be threaded in to the existing fastener holes to drive the sections apart (Appendix Figure 33, 34). Standard 5/8" bolts could be

adapted for this purpose by making some simple step-down modifications in diameter along their length.

### **Manufacturing Procedure**

The manufacturing processes of the molds are outlined below (relevant images available in Appendix Figures 31-45):

1. Bandsaw cutting of aluminum blocks for Section 1-8. The aluminum slabs used came in an unusual shape; cuts were first done to remove excess material, leaving a square block of rough oversized dimensions. In one case, a bandsaw cut was also done to trim a block to thickness to avoid excessive facing operations.
2. Manual milling of blocks to square them to the correct length, width, and height. The blocks were first faced to the correct thickness, machining both sides to ensure smooth surfaces. The side faces of the blocks were then faced to square the blocks and make their lengths and widths equal. For the four main sections, a double vice setup including an angle plate and clamps was used to ensure adequate rigidity (see Appendix). The side features to secure Sections 5-8 were also drilled as this time.
3. Drilling/boring of fastener holes using manual mill. All  $\frac{1}{2}$ " holes for the shoulder bolts were first drilled to a lower diameter and then reamed to ensure tight tolerances. All countersink features for bolt heads were done by plugging with end mills. Slits were machined into section edges for mold release. Because this method is much easier than machining custom bolts, it was tried first, and ultimately turned out to be sufficient.
4. Tapping of required  $\frac{1}{4}$ ",  $\frac{3}{8}$ ", and  $\frac{5}{8}$ " threads.
5. CNC machining of Section 2, side 1. Done using a  $\frac{5}{8}$ " bullnose end mill with a 0.09" corner radius, 5" overall length. Block was dialed in square to the table and zeroed, with toolpaths for roughing, rest roughing and finishing. The rest roughing toolpath was done because roughing leaves a "staircase" like pattern on the outside contours; these should be smoothed out so that the finishing passes remove a relatively consistent amount of material.
6. CNC machining of Section 3. This was done by bolting on to Section 2 while still on the table. It was important that the CNC machining was done sequentially with each block bolted on top of the other in the machine. This allowed the same original datum from zeroing on Section 2 to be maintained so that each profile was machined entirely with respect to it. If each piece were to be machined separately, there would be an increased likelihood that the seams at the profile would not match up perfectly when sections were joined because of small errors re-zeroing and dialing the parts. A 2" face mill was used for roughing, ramping in to each stepdown helically. Rest roughing and finishing were once again done with the  $\frac{5}{8}$ " end mill.
7. CNC machining of Section 4, by attaching to Section 3. Because of the thickness of this part, the face mill could not reach down to the full depth of the part. After this point, the  $\frac{5}{8}$ " mill carried on the remainder of the roughing, as well as the rest roughing and finishing.
8. CNC machining of Section 2, side 2. The same operations used in Step 5 were repeated on the opposite side of Section 2.
9. CNC machining of Section 4, by attaching to Section 2. Like Section 3, the thickness did not allow the face mill to be used for all roughing. Also, the  $\frac{5}{8}$ " end mill was extended to reach down a full 4" from the collet. Step downs and step overs were slightly reduced in case of chattering with this reduced rigidity.

10. Sanding and polishing of rim surfaces. Sanding was done with sandpaper of 150, 220, 400, and 600 grits. Relatively good finish was obtained from machining such that excessive sanding was not required except where rougher “staircase” shaped contours occurred, which required 40 and 100 grit sandpapers. The parts were then cleaned using a polishing attachment and compound.

## 2.3 CARBON LAYUP PROCESS AND PROTOTYPE

---

### Layup procedure

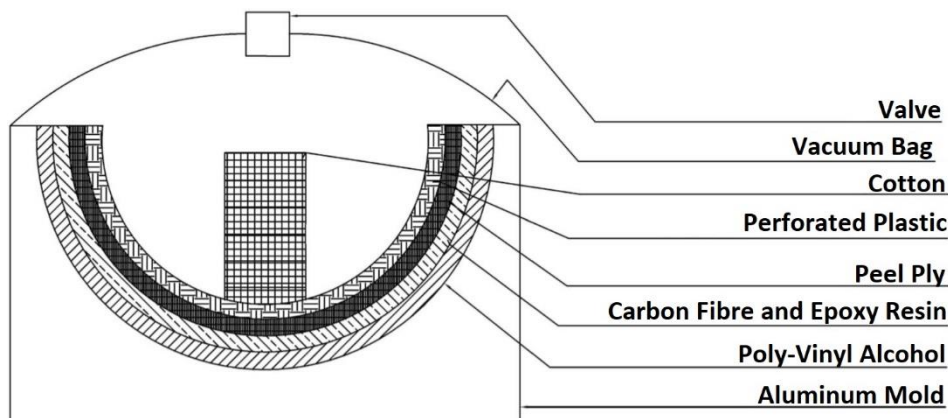


Figure 21: Carbon Fibre Layup Schematic

The physical creation of the rim begins with the layup process. First, the surface of the mold is degreased with isopropyl alcohol. A layer of PVA mold release must be applied to the mold using a brush or cloth. After the PVA has dried for at least 15 minutes, a thin layer of epoxy is applied to the surface and the first layer of carbon fibre is laid down. After the carbon fibre is secure, a layer of epoxy is applied using a dabbing motion to the carbon fibre. This process is repeated until the required number of composite layers is achieved. Peel ply is set on top of the carbon fibre-epoxy stack. The peel ply layer performs multiple functions: it absorbs and disperses epoxy and separates the above layers from the CF part. Above the peel ply comes a layer of perforated plastic. The holes in the plastic allow the epoxy to disperse at a controlled rate when the vacuum pump is running. Any extra epoxy is well dispersed and is absorbed by the cotton layer. This cotton layer prevents any extra epoxy from pooling in one area of the piece and prevents epoxy from reaching and destroying the valve. The last layer is the vacuum bag which is secured to the mold base using double sided tape. This bag has a small hole cut into the top of it to insert the valve for the vacuum pump hose.

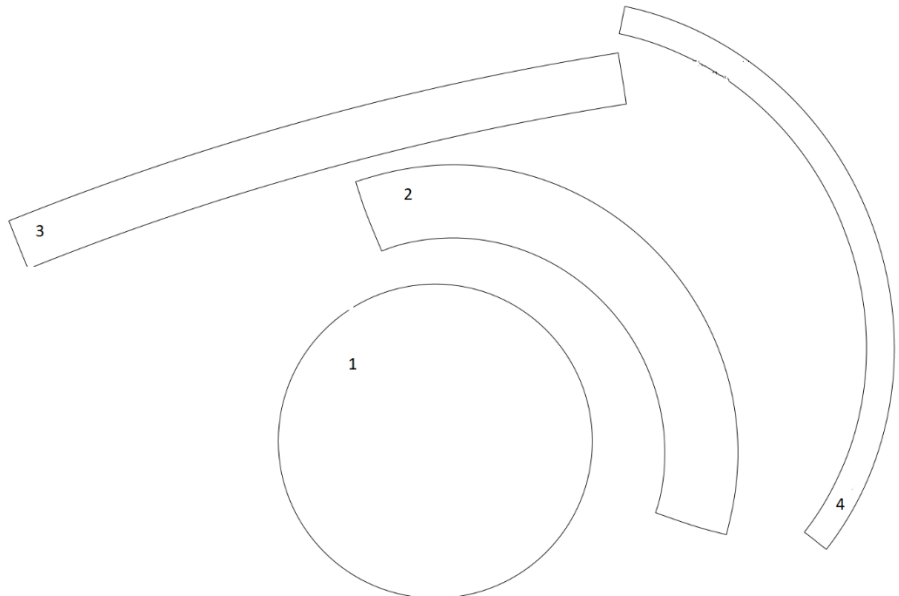


Figure 22: Carbon Fibre Test Piece Using a Safety Hat as a Mold

To practice this detailed process, test pieces were made using a 1x1 weave carbon fibre found in the race shop. Using a bump cap as a mold, the layup process was practiced. The CF bump cap was made using only two layers of carbon fibre and could withstand a large amount of force. Four pleats were cut into the pieces of carbon fibre to allow proper draping of the composite. The same method was used when creating the carbon fibre pieces for the rim. Additional strips of carbon fibre can be used to create an appropriately thick tire bead for the rim. These extra layers also ensure the bead will not fray and fail when in use. At the edge of the tire bead, the layers end slightly below the edge of the mold surface so that the vacuum bag does not catch the carbon and peel it downward off the mold.

When the time came to make a prototype carbon fibre rim with the aluminum mold, templates were created using the flatten tool in SolidWorks and these were printed at a 1:1 scale onto poster board. Carbon fibre shapes were cut out by taping around these templates, then cutting through the centre of the tape. Cutting through the centre of the tape ensures a slightly oversized part that will overlap with the parts around it, and the tape also keeps CF fibres from being pulled out of the correct orientation.

The outer shell of the prototype rim was made with bands of CF that built up from the bottom of the mold (see Figures 23 and 24 below). Using bands of carbon fibre was an acceptable option but was very time consuming and required extreme care when applying the strips of carbon to the mold, since the first layers tended to slip down to the bottom of the mold as more layers were applied on top.



*Figure 23: Banded-style layup shapes. Shapes Were Applied in the Numbered Order Which Built up the CF Part from the Bottom to the Top. The Arcs 2, 3, and 4 are Half-Length in Order to Fit on 18" x 22" Sheets of Paper*

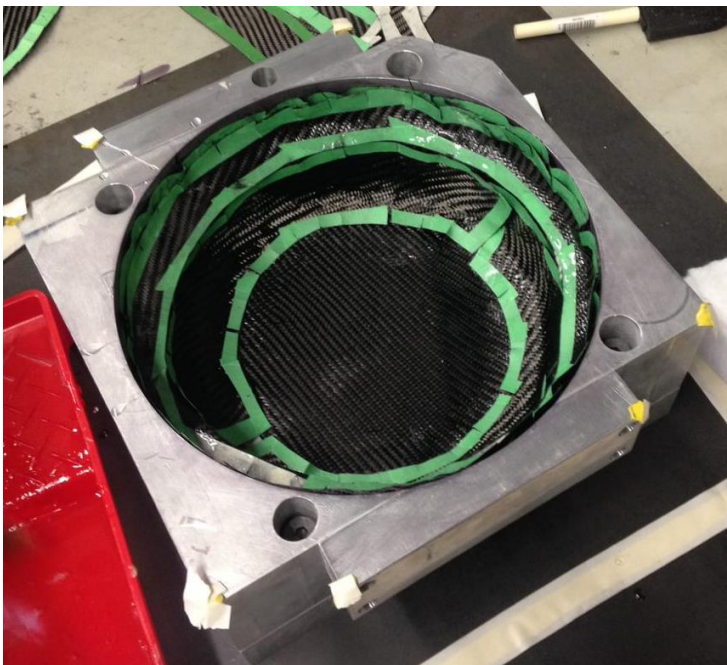


*Figure 24: Banded-Style Layup in Progress on the Mold*

The inner half of the rim was created with a central circle and radial slices (see figures 25 and 26 below). In order to ensure that the overlapping areas of the slices would not be a weak point, each layer of this template was oriented 45 degrees from the previous. Laying up the carbon in a radial pattern proved easier than the bands used for the previous section. The half of the rim created using radial slices had an improved surface finish compared to the half of the rim created with the vertical bands. Building up the carbon using these radial slices is the recommended method for future layups performed by the Guelph FSAE team. It is preferable to use as few individual pieces with as few relief cuts as possible, as

the strength of the composite relies on the continuity of the carbon. With each layup style, relief cuts were made into the cut-outs where they were required to lay flat over a curved surface, as discussed above with the bump cap.

Note that only six layers of carbon were used in the creation of the prototype rim, as this part is intended only as a proof of concept.

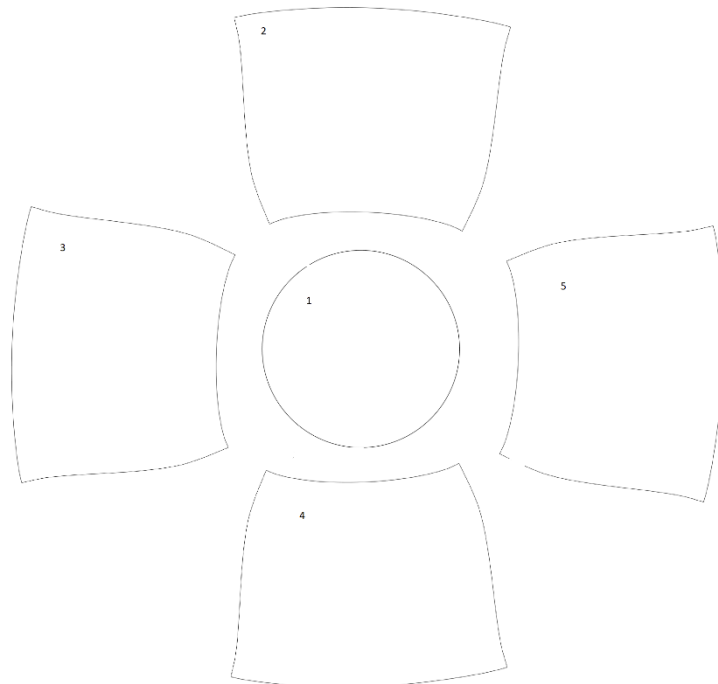


Figure 25: Radial Slice-Style Layup Shapes. Shapes Were Applied in the Numbered Order Which Built out the CF Part Radially. Shapes 2, 3, 4, and 5 Were Offset by 45 Degrees from the Layer Above and Below in Order to Ensure No Weak Points

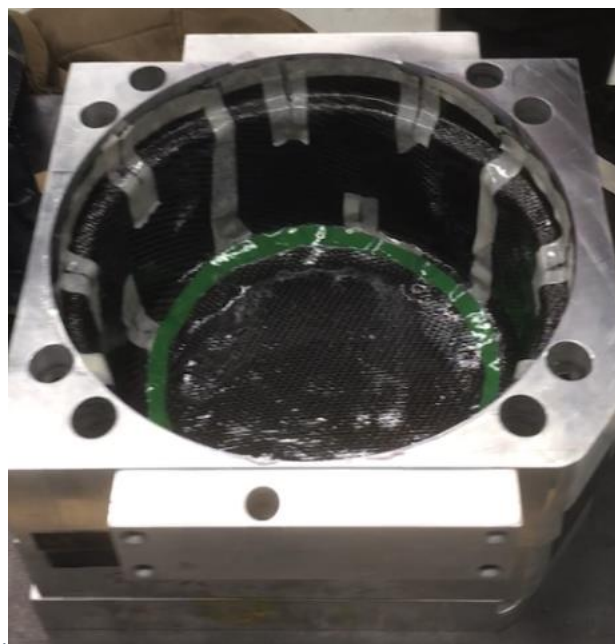
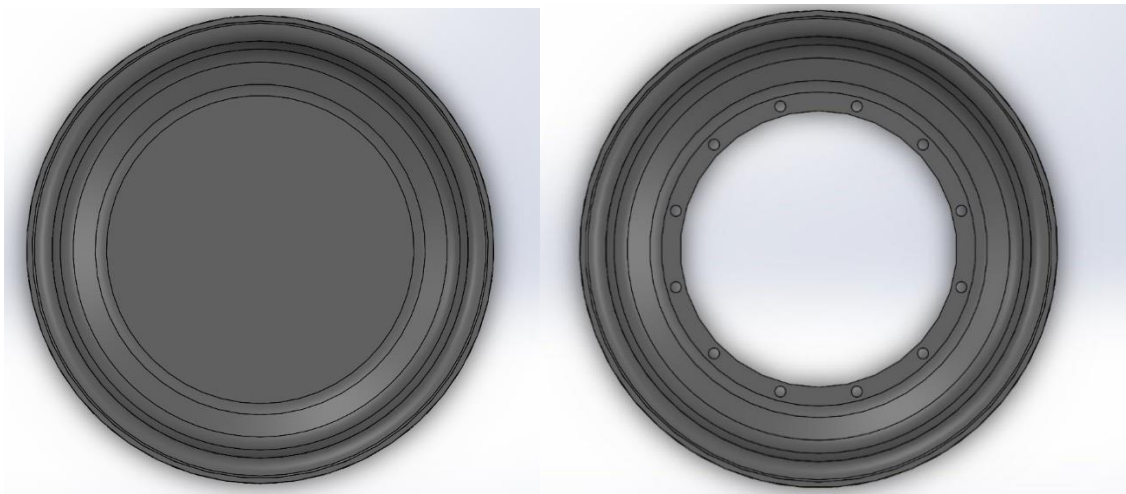


Figure 26: Radial-Style Layup in Progress on the Mold.

## Post-Machining and Finishing



*Figure 27: Features to be Machined*

There are some precautions necessary for the machining of carbon fibre in terms of both safety and the quality of the machining. Machining carbon produces fine particulates that are hazardous to breathe in, therefore it must be done with the use of either an extraction system or dust binding coolant. This means that the machining facilities available in the School of Engineering, such as the CNC mill, are not suitable. The machining has been done by hand to produce a prototype part, with the extractor in the Gryphon Racing shop used during the process.

Special care should also be taken during this process because of carbon's abrasiveness and sensitivity to machining conditions. In industry, typically diamond coated carbide tooling is used because high speed steel (HSS) or uncoated carbide will wear at an accelerated rate. Wear is further increased if the feeds and speeds are either too high or low. For drilling, standard 118-degree angle drill bits are known to cause delamination of the lamina when making holes. Drill bits with elliptical profiles and other specialized geometry can be used to avoid delamination because they apply less downward pressure in the drilling process. [11]

The team has chosen not to make the extra investment into this tooling as it was determined to be cost prohibitive. Also, although this equipment is most suitable, regardless it can still be quickly ruined when used incorrectly by inexperienced operators. Drilling of the 12 bolt holes has been carried out successfully by sharpening a standard drill bit to a 60-degree angle. In the future, an additional hole for the pressure valve can also be drilled in this manner.

In the future, it is recommended to use the CNC router in the Gryphon Racing shop for carbon machining. Modifications would need to be made for this to be possible, including removal of the table or a redesign of the router fixture to accommodate the height of the parts. CNC machining these features with each part still in the mold would improve accuracy and ensure proper concentricity.

With machining completed, the parts are then finished by lightly sanding with fine sandpaper, applying a gloss clear coat to improve the appearance of visible surfaces, and sealing them together. The final prototype is shown below.



Figure 28: Final Prototype

## 3.0 UNCERTAINTIES AND RISKS

---

There are several risks associated with this project. They are all dependent on the preparation and care taken both before and during the process. With proper research, safety equipment, and being attentive to the process, most of these risks can be removed.

### **Carbon Fibre Research**

Research must be conducted long before the layup process occurs to ensure the correct type of carbon fibre is used. If an incorrect weave is used (i.e. using unidirectional when twill should be used) the carbon fibre will not behave as intended, leading to difficulty in adhering to contours during layup or incorrect strength properties due to orientation. The physical properties of the cured carbon fibre are highly dependent on the type of weave used.

### **Quality of Epoxy**

The quality of the epoxy resin and hardener must also be considered before the layup process begins. If a low-quality epoxy is utilized, the carbon fibre part will not offer the anticipated strength and stiffness properties and will delaminate sooner than expected. The epoxy and hardener must also be mixed for an ample amount of time before it can be applied to the carbon fibre. If insufficient mixing occurs, there will be a lack of bonding between the two fluids and once again, the expected properties will not be achieved.

### **Caution During Layup**

Extra care must be taken when completing the layup process. The pieces must not overlap too much or else the thickness will be uneven, and the strength of the overall piece may change. The correct

amount of cotton must be used or else proper contact between the carbon and the suction of the vacuum will not be met and the geometry of the piece will be skewed. If too much epoxy is added, it will pool in areas. If there is not ample PVA, epoxy may adhere to the mold and there is an increased risk of air bubbles.

### **Application of PVA**

If ample PVA is not applied, epoxy will adhere to the mold as well as the carbon fibre and could potentially lead to the inability to release the part from the mold. Even in the case that the part was released, large portions of epoxy could remain on the mold. This residual epoxy must be fully cleaned using acetone and sandpaper to ensure the geometry (especially the tire bead) is consistent between uses.

### **Degradation of Aluminum**

Steel shoulder bolts were used to connect the separate pieces of the mold together. Because the mold was formed out of aluminum, which is much softer than steel, there is a risk of stripping threads if the bolts are overtightened repeatedly. Also, the molds require some sanding after making each part when removing epoxy left behind. This should be done with care, using acetone to ease the process.

### **Carbon Fibre Strength Post-Machining**

Carbon fibre gets its strength from the entwinement of long carbon chains. When the carbon is machined, these long carbon chains are disrupted and the physical properties of the carbon changes at the location of machining. The epoxy generally adds enough strength to the fibre matrix to overcome this strength difference.

### **Hazards of Carbon Fibre**

Carbon fibre releases small particles into the air when it is cut or machined. There is a risk of these particles entering the lungs and causing tissue damage. There is also a risk of the fibres embedding themselves into skin causing itchiness, splinters, or both. For these reasons it is important to wear proper personal protective equipment and take proper precautions before working with the carbon fibre. Proper equipment includes respirators and gloves to prevent inhalation and splintering. Before working with carbon fibre ensure that any carbon fibre particulates will be extracted by either a ventilation system or a specialized coolant.

## **4.0 CONCLUSIONS AND RECOMMENDATIONS**

---

A reduction of mass in the rims was necessary to improve vehicle performance of the Gryphon Racing FSAE car as it reduced rotational inertia, unsprung mass, yaw inertia, and overall vehicle mass. 2x2 twill weave carbon fibre in combination with high quality structural resin has been deemed the best material choice due to the high strength to weight ratio and ease of draping on complex surfaces.

A custom rim profile has been designed with consideration of suspension design criteria, ease of mold release, and minimization of stress concentrations. Detailed structural analysis of the composite rim was completed to determine the required layering and orientations of the carbon laminae. Load cases for cornering, longitudinal acceleration, road bumps, and over-pressurized tires were considered.

A modular female aluminum mold has been designed. This type of mold was specified because it provides high dimensional accuracy on critical surfaces and could be feasibly machined using SOE facilities. This design was successfully executed, and the finished mold assembly is fully functional. A complete prototype rim was created, including the necessary post machining features.

The success of this project has been measured by the ability to carry out a comprehensive rim design process, as well as manufacture a full mold assembly and prototype rim to prove the feasibility of the design. During the period of this project, skills such as vehicle dynamics and MATLAB, materials testing, structural analysis and ANSYS, solid modeling, and manufacturing were applied to cover all relevant aspects of this engineering problem. With the successful execution of the intended goals, this project is now considered complete.

Recommendations for the future advancement and implementation of this design are as follows. The carbon fibre layup process of the rim should be further refined to ensure proper and uniform adherence to the mold surfaces throughout the entirety of the part. One approach to this would be to change the shape of the excess cotton layers added underneath the vacuum valve, such that this material does not prevent the vacuum bag from being drawn into the part's corners. It would also be sensible to perform destructive testing on the prototype rim, to provide a final verification of the ANSYS model. This would shed much more light on the accuracy of the modeling conditions than the previously done tensile tests, which can verify material properties but not give any information regarding the possible effects of layer interruption and overlap throughout the part, and the addition of tape to layer edges. The FEA model can be modified to have six layers like the prototype part relatively easily. It is also recommended to find a method of post machining the rim features more accurately on a CNC mill or router as discussed in the post-machining section. When a tire is added to the rim, it should be checked that it is airtight, and not out of round or bent.

## 5.0 REFERENCES

---

- [1] Adam, H. "Carbon Fibre in Automotive Applications". *Materials and Design*. Vol 13. Iss 4-6. PP 349-355. December 1997. DOI: [https://doi.org/10.1016/S0261-3069\(97\)00076-9](https://doi.org/10.1016/S0261-3069(97)00076-9)
- [2] "Aeropoxy PR2032 + PH3663 (Gallon kit)". Composites Canada. March 28, 2019. URL: <https://shop.compositescanada.com/#/product/AE2032-63-X>
- [3] "Aluminum Wheels vs. Magnesium Wheels". CarsDirect. February 21, 2012. URL: <https://www.carsdirect.com/aftermarket-parts/pros-and-cons-of-magnesium-wheels>
- [4] "Aluminium vs. Carbon Fiber - Comparison of Materials." DexCraft. October 7, 2015. URL: <http://www.dexcraft.com/articles/carbon-fiber-composites/aluminium-vs-carbon-fiber-comparison-of-materials/>
- [5] Bastow, D., Howard, G., Whitehead, J. "Car Suspension and Handling". Feb 2004. Available: [http://sutlib2.sut.ac.th/sut\\_contents/H96323.pdf](http://sutlib2.sut.ac.th/sut_contents/H96323.pdf)
- [6] Chapman, Matthew K. "Development of a Composite Wheel Rim for an FSAE Car". University of New South Wales. 2011. Print.
- [7] Drakonakis, V., Seferis, J., Doumanidis, C. "Curing Pressure Influence of Out or Enclave Processing on Structural Composites for Commercial Aviation". *Advances in Material Science and Engineering*. Vol 13. Sept 2012. Available: <https://www.hindawi.com/journals/amse/2013/356824/>
- [8] "Fabric Styles". Advanced Composite Materials inc. 2016. URL: [http://www.a-c-m.com/fabric\\_styles/default.html](http://www.a-c-m.com/fabric_styles/default.html)
- [9] Hyer, Michael. "Stress Analysis of Fiber Reinforced Composite Materials". Boston: McGraw-Hill. 1998. Print.
- [10] Luo, M. "Magnesium: Current and Potential Automotive Applications". *Journal of Minerals, Metals, and Materials Society*. 54:42. Feb 2002. Available: <https://doi.org/10.1007/BF02701073>
- [11] MacArthur, Mike. "How to Machine Carbon Fibre and Today's Difficult Composites". Youtube. Feb 10, 2012. URL: [https://www.youtube.com/watch?v=OlaL\\_epxjoA](https://www.youtube.com/watch?v=OlaL_epxjoA).
- [12] Marker, T. "Evaluating the Flammability of Various Magnesium Alloys During Laboratory- and Full-Scale Aircraft Fire Tests" US DOT FAA. January 2013. Available: <https://www.fire.tc.faa.gov/pdf/ar11-13.pdf>

## 6.0 APPENDICES

---

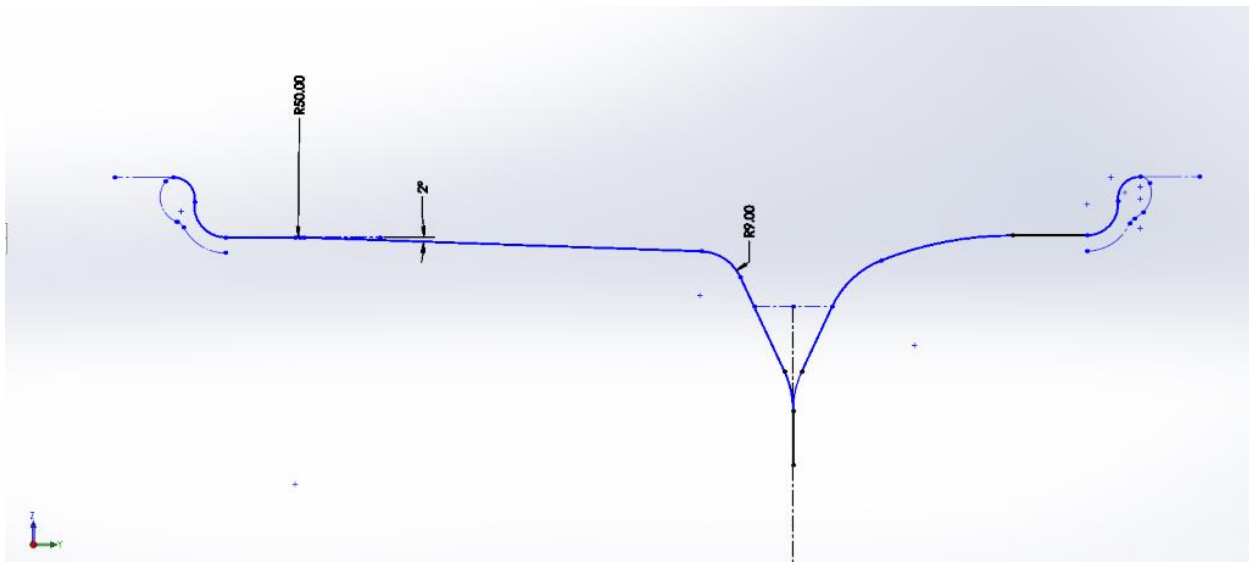


Figure 29: Rim Profile of Final Design

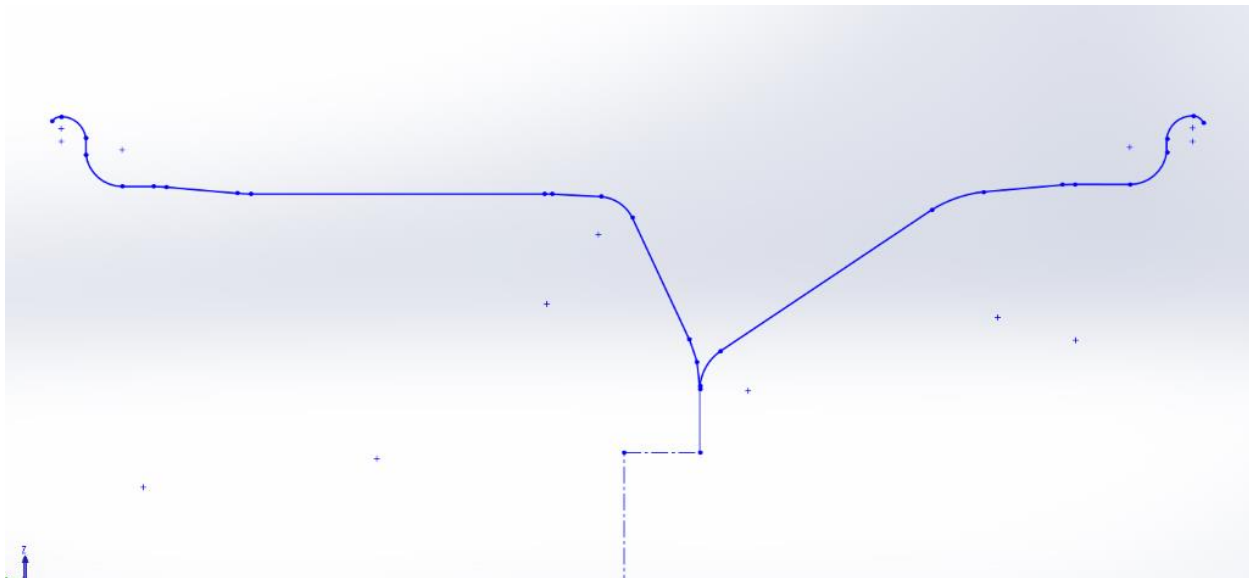


Figure 30: Rim Profile of Original Aluminum Design

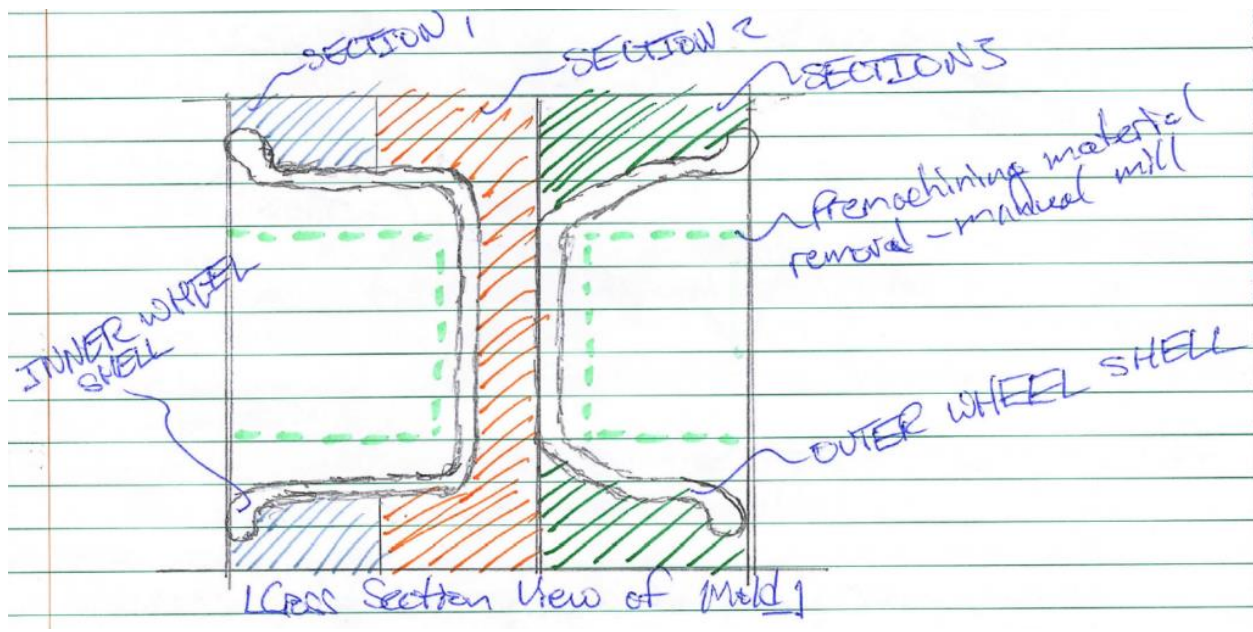


Figure 31: Section View of Mold Version 1

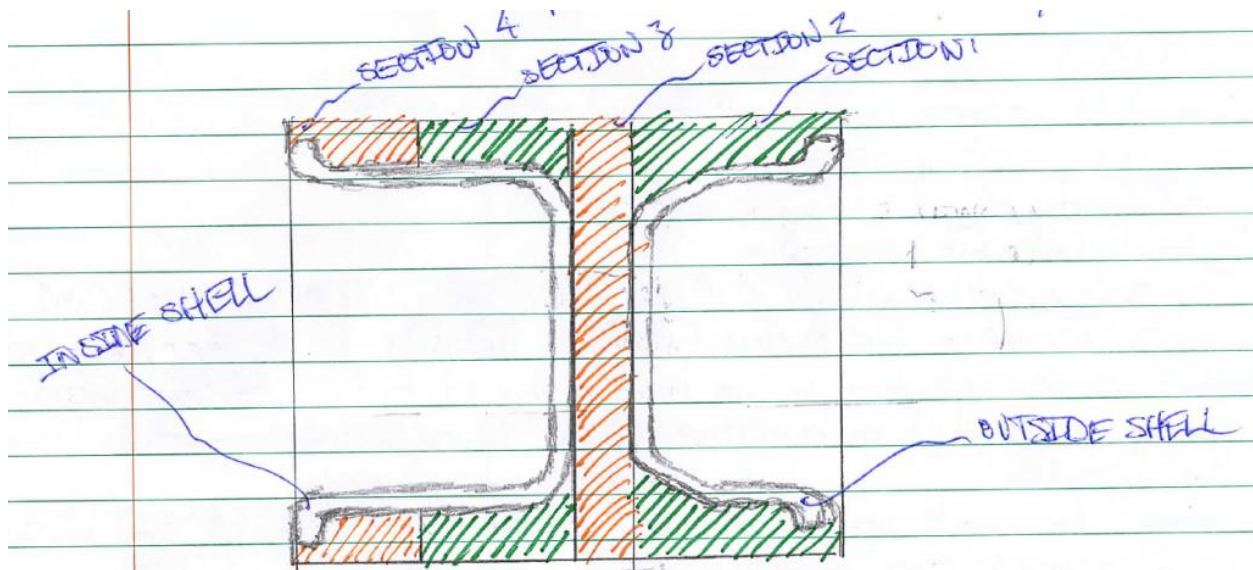


Figure 32: Section View of Mold Version 2

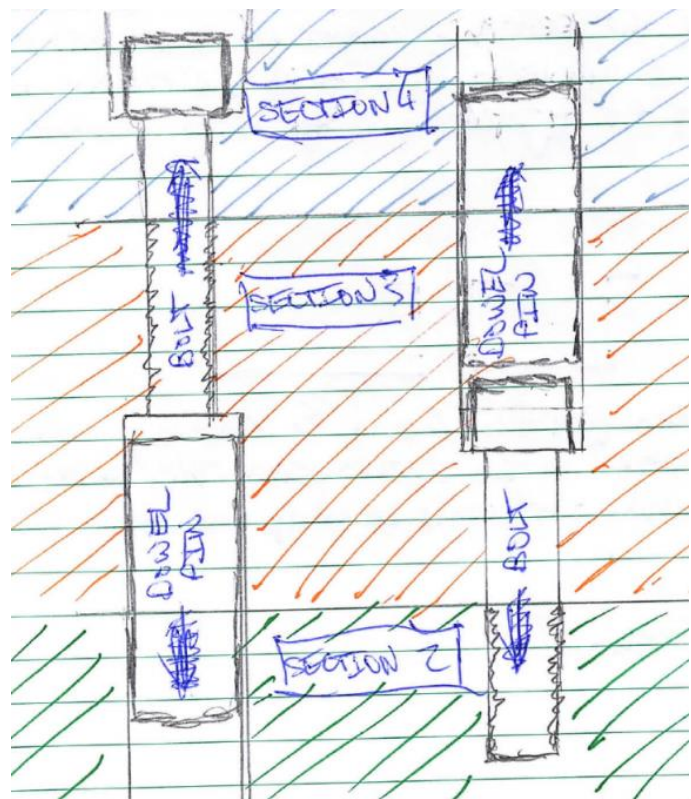


Figure 33: Sketched Layout of Fastening Features (Version 2)

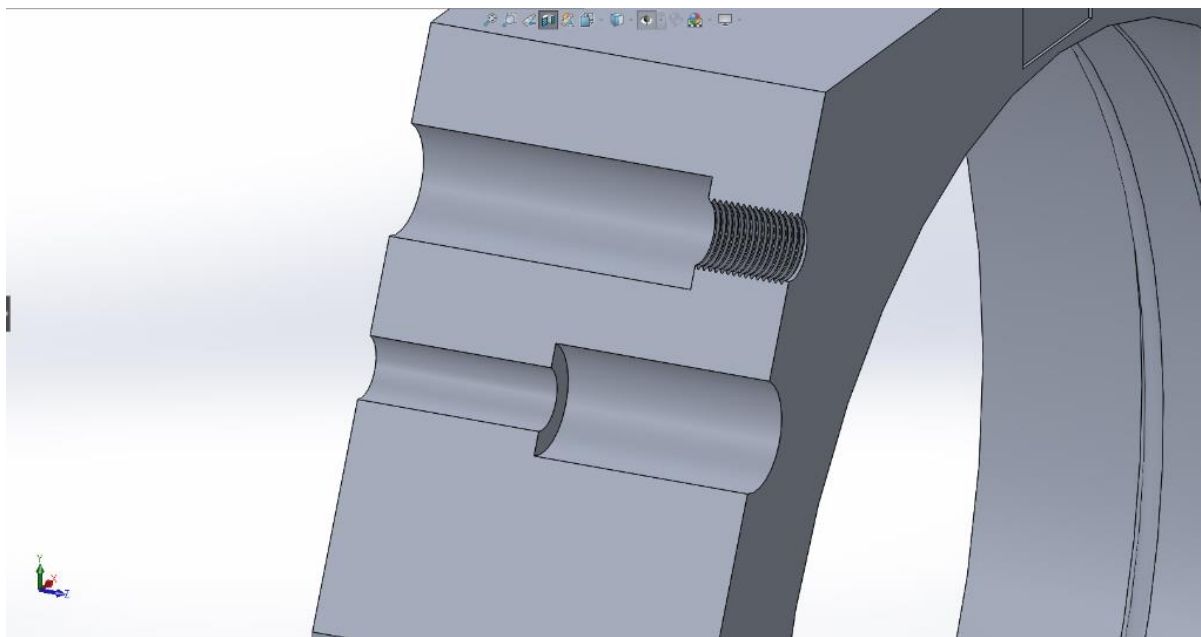


Figure 34: CAD Layout of Fastening Features (Version 2)

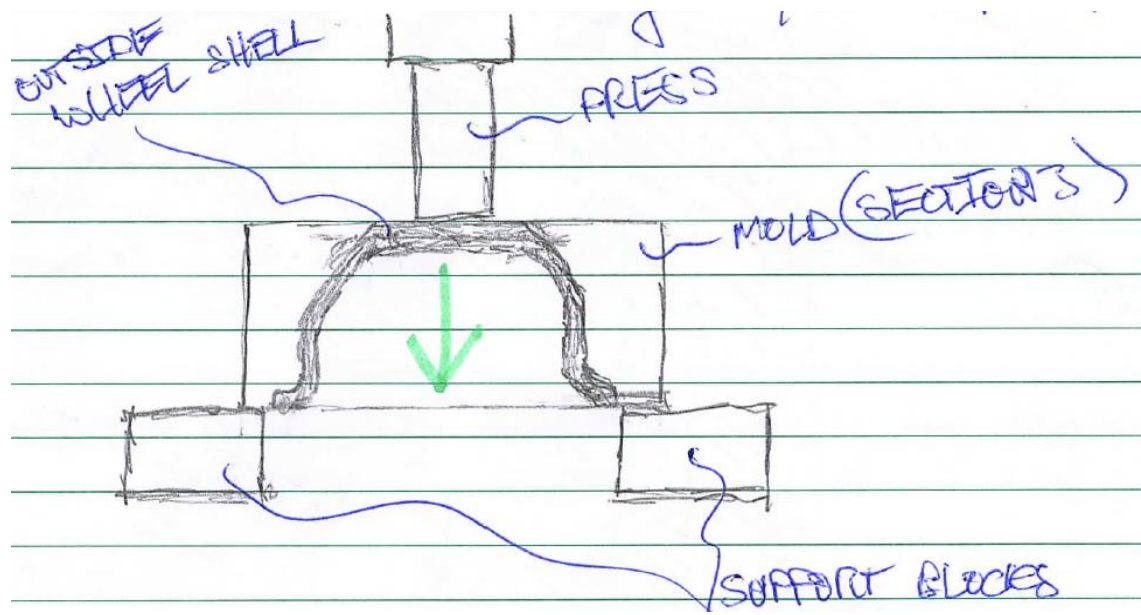


Figure 35: Diagram of Mold Removal Using a Hydraulic Press

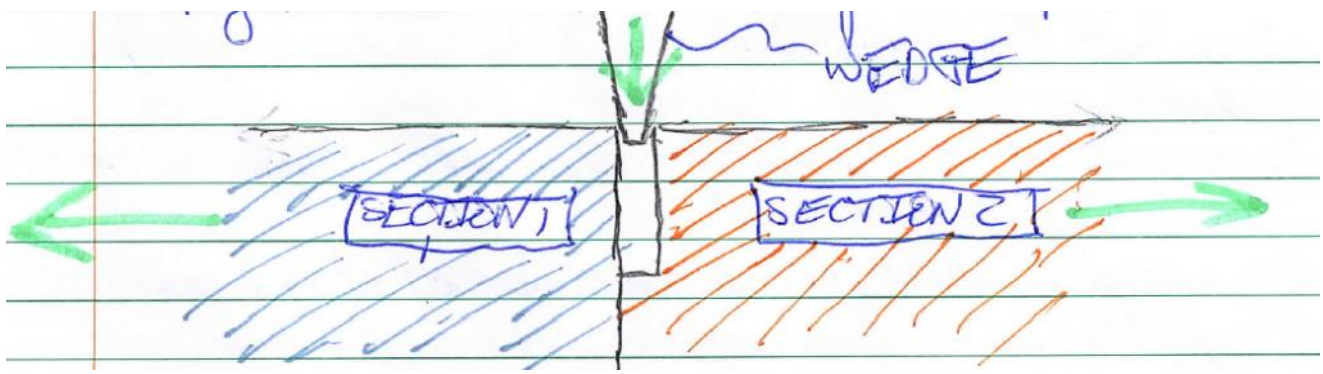


Figure 36: Diagram of Section Separation

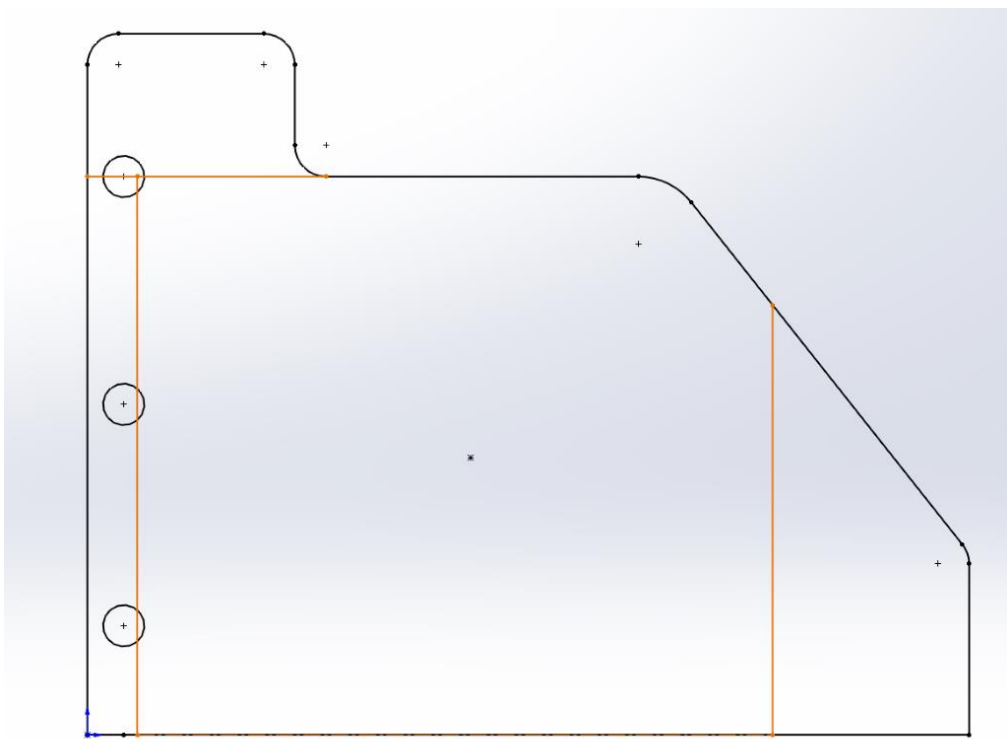


Figure 37: Band Saw Cuts to be made in Aluminum Block

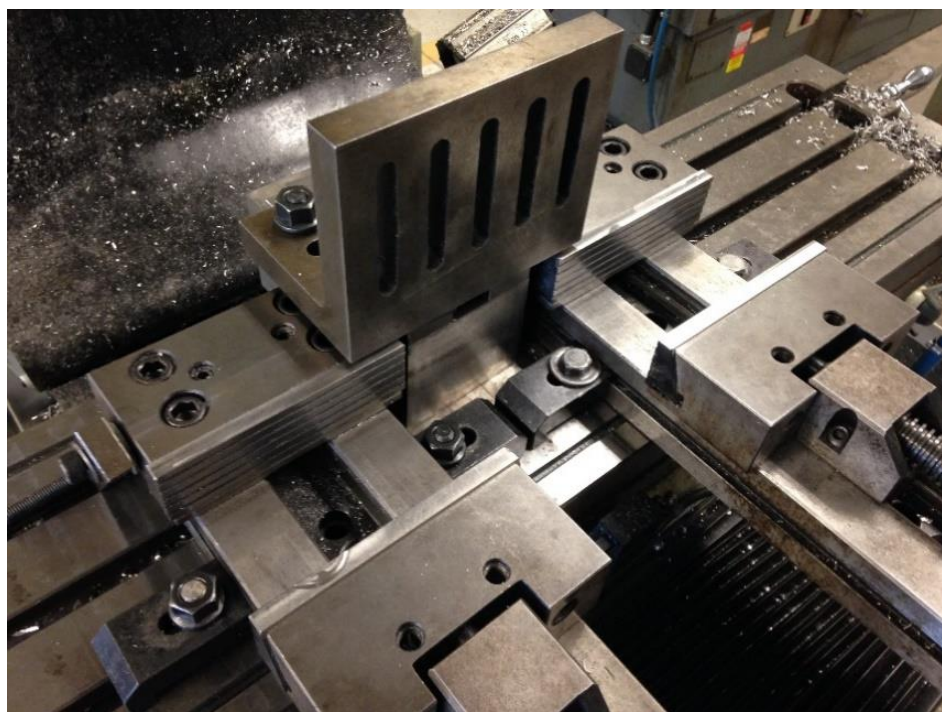


Figure 38: Machining Setup for Machining of Block Side Faces



Figure 39: Machining of Block Side Faces



Figure 40: Main Sections after Facing

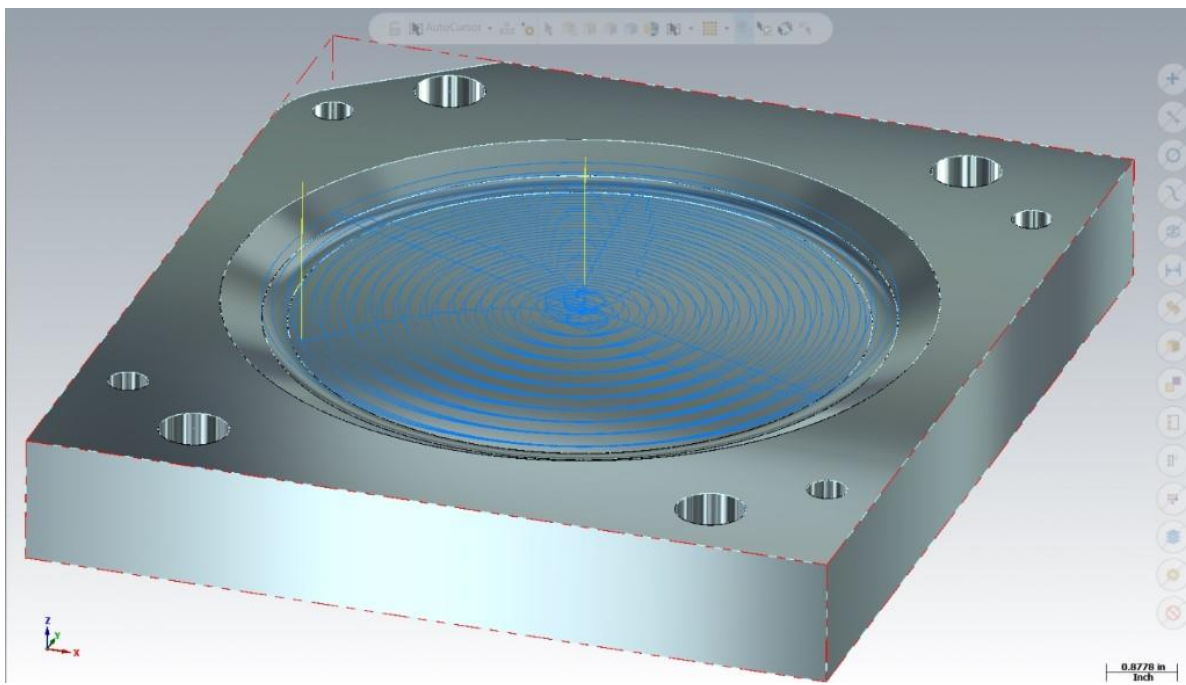


Figure 41: Roughing Tool Path for Section 2

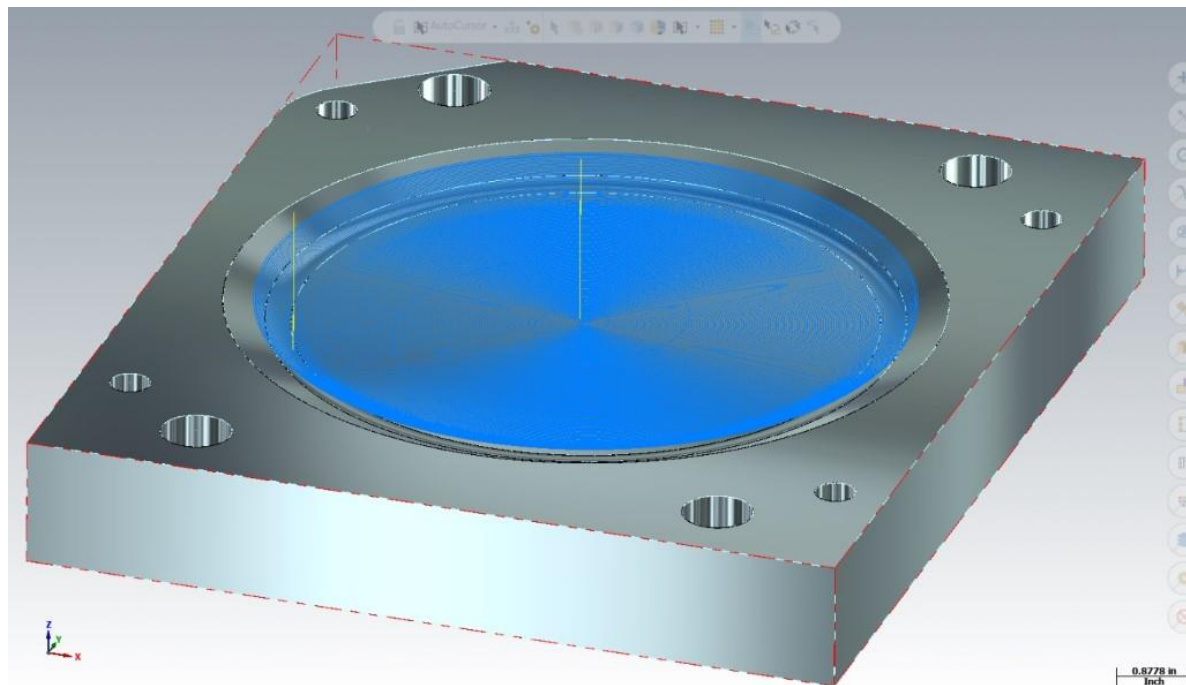


Figure 42: Finishing Tool Path for Section 2

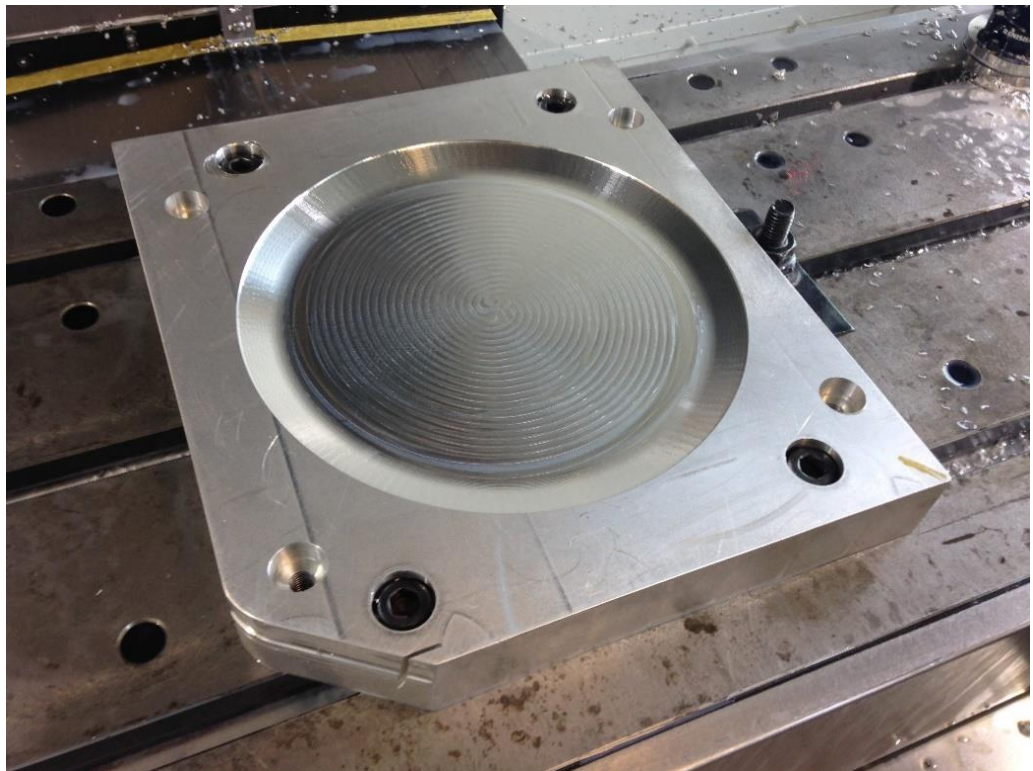


Figure 43: Section 2 after CNC Machining

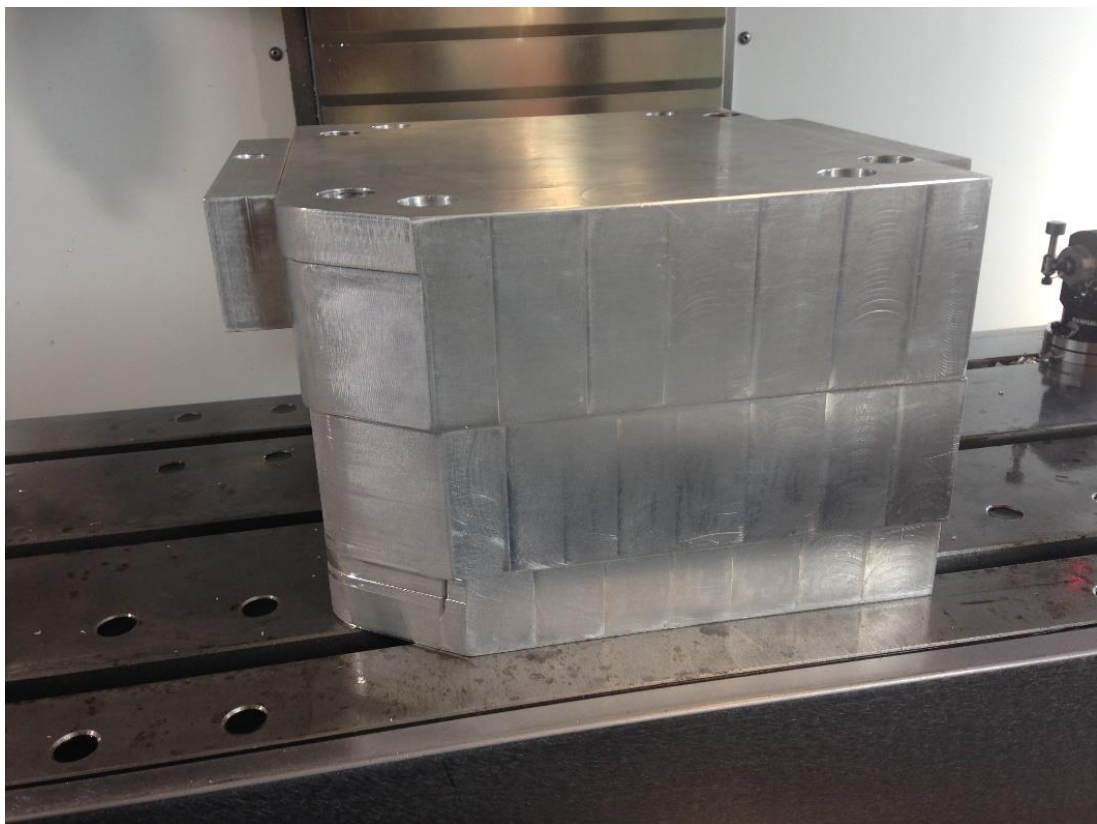


Figure 44: Section 4 before CNC Machining, with Section 3 and Section 2 Below.

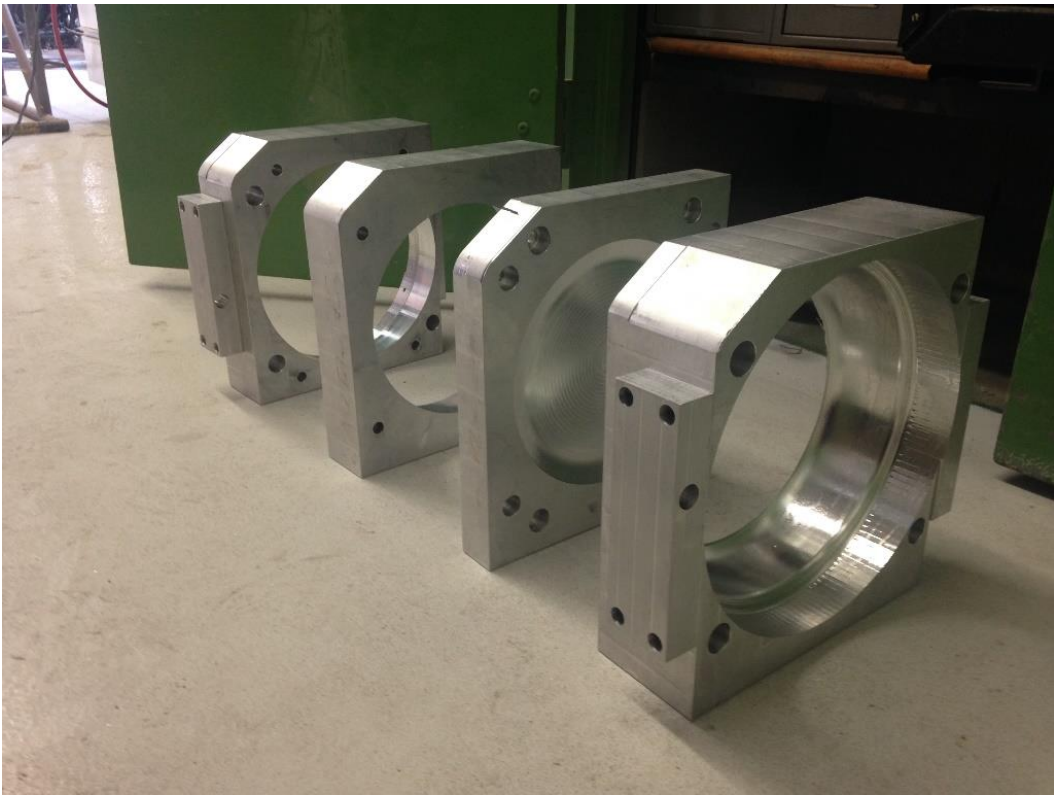


Figure 45: Mold Sections after CNC Machining

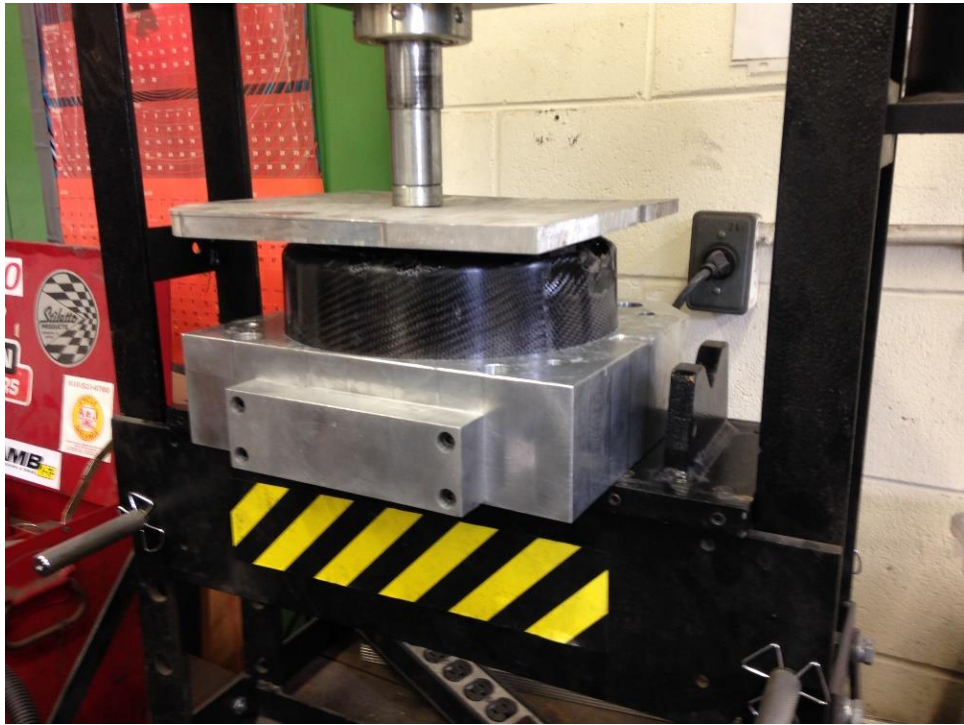


Figure 46: Mold Release of Finished Outer Shell

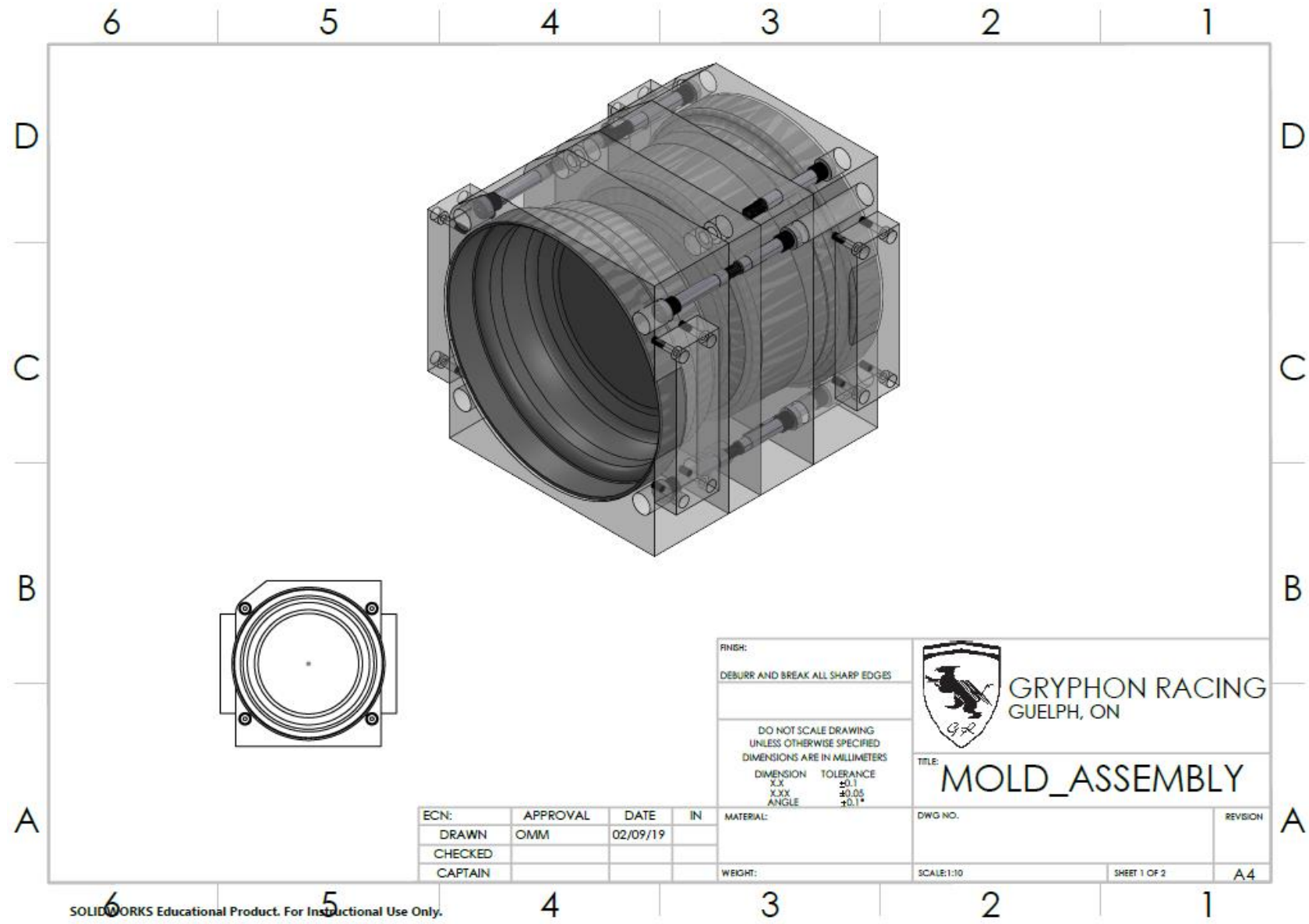


Figure 47: Drawing of Mold Assembly, First Page

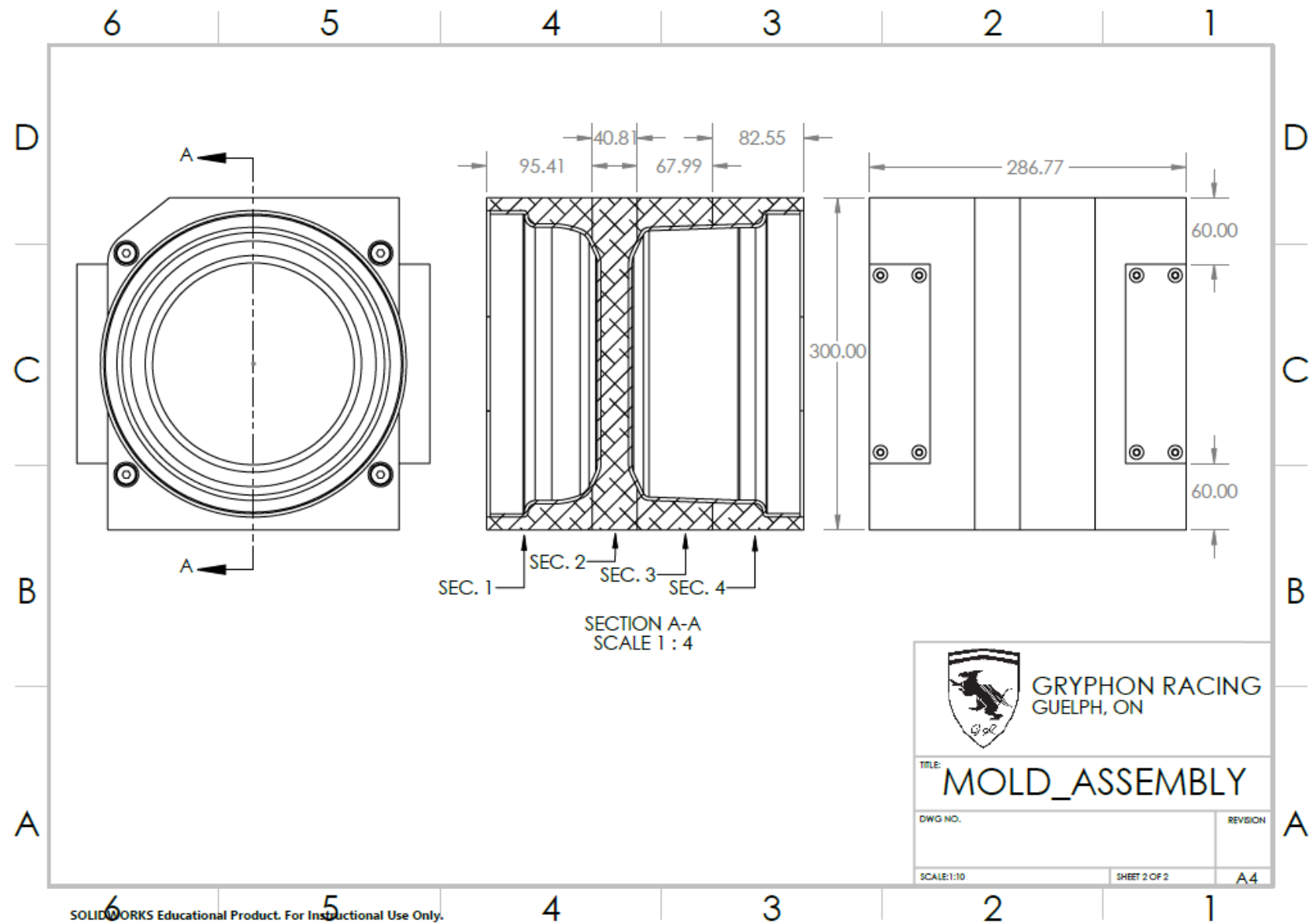


Figure 48: Drawing of Mold Assembly, Second Page

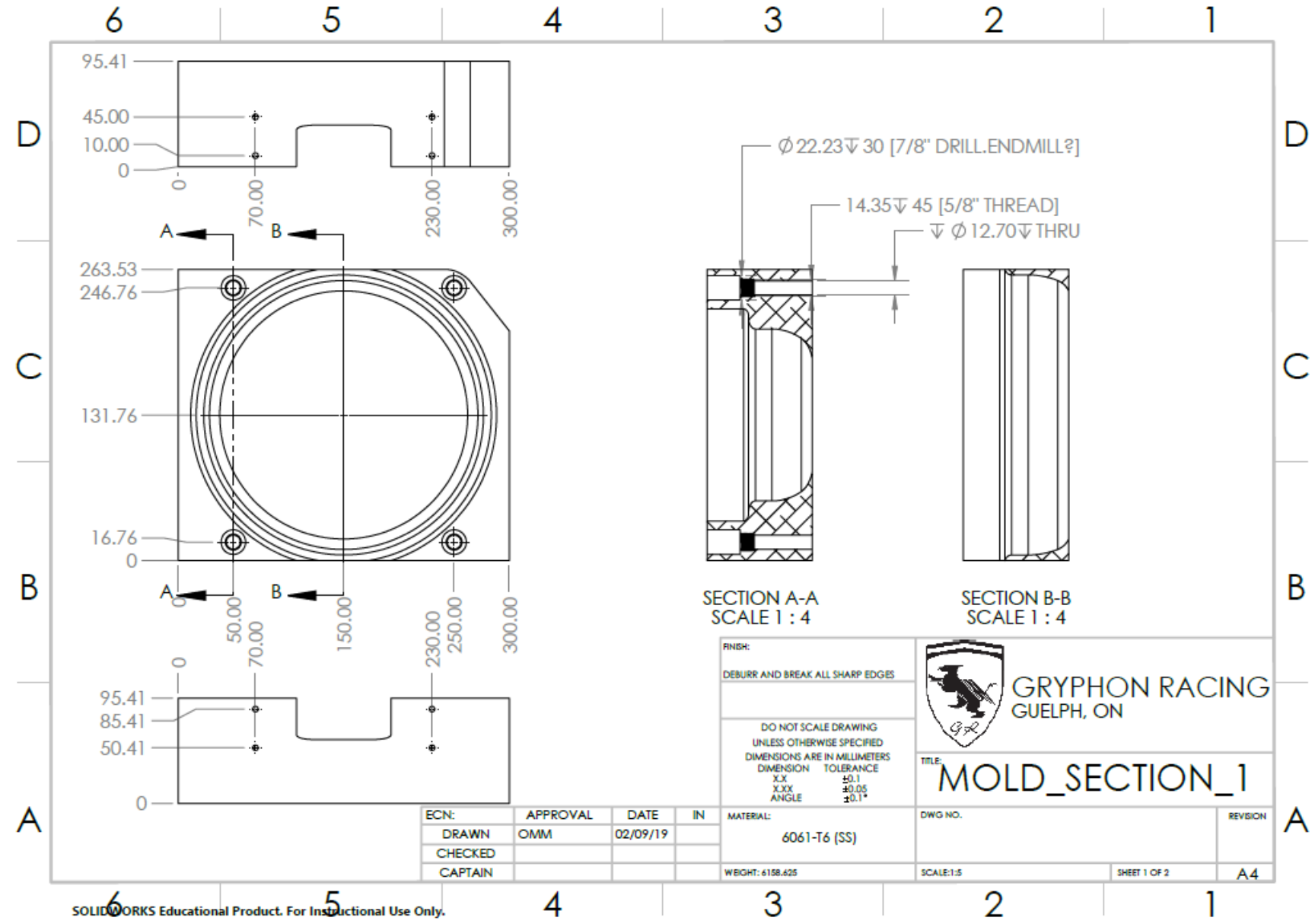


Figure 49: Drawing for Mold Section 1

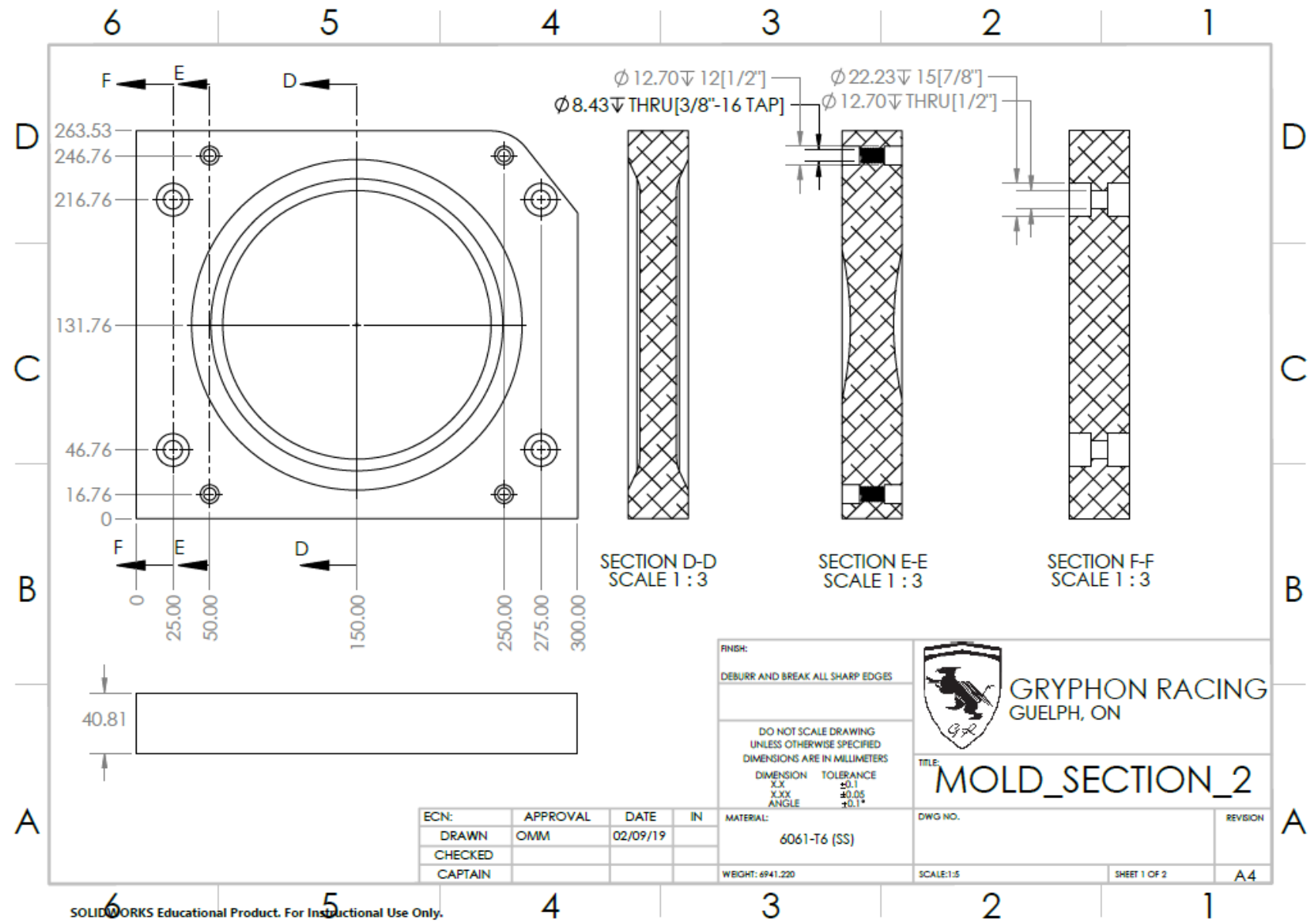


Figure 50: Drawing for Mold Section 2

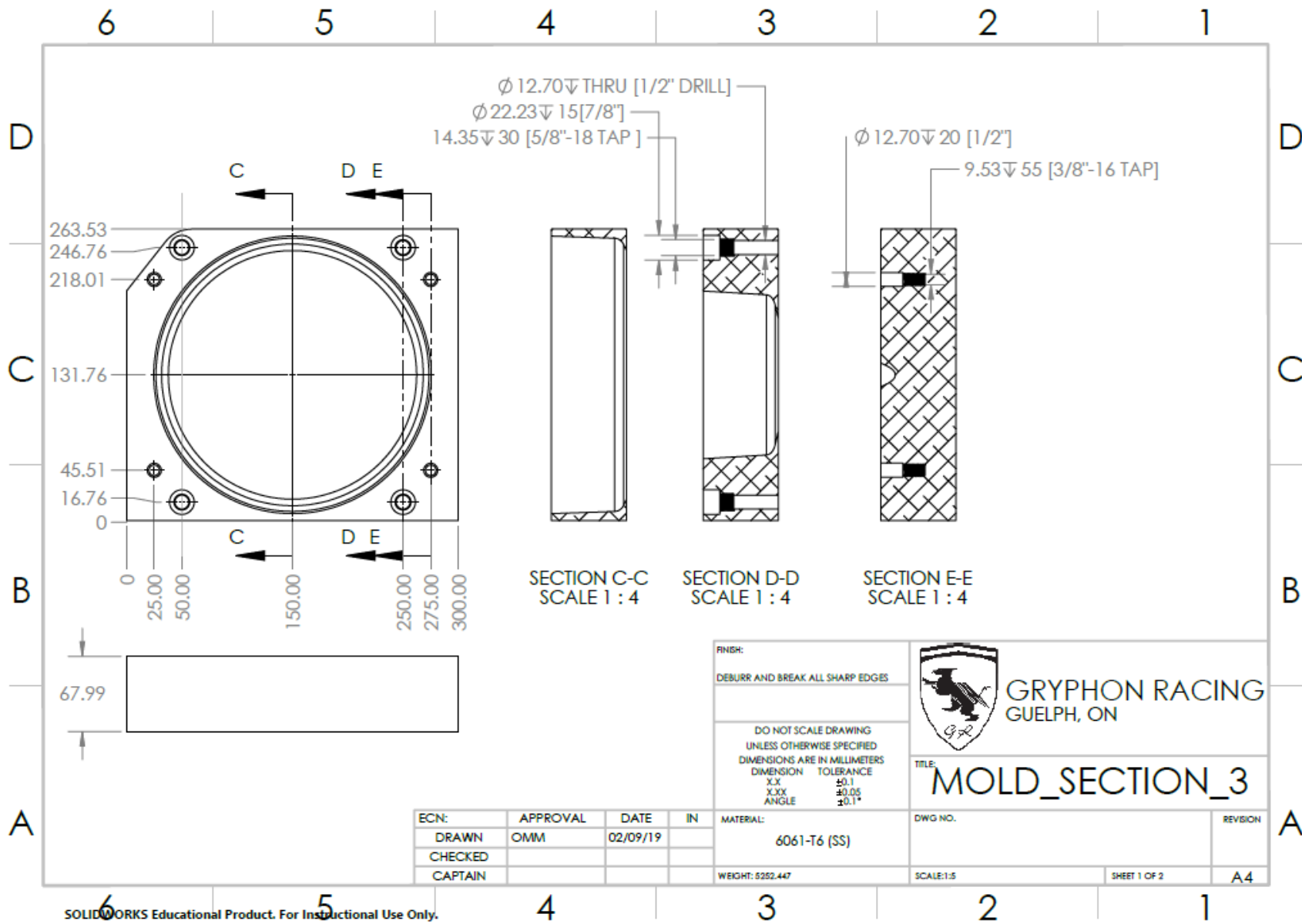
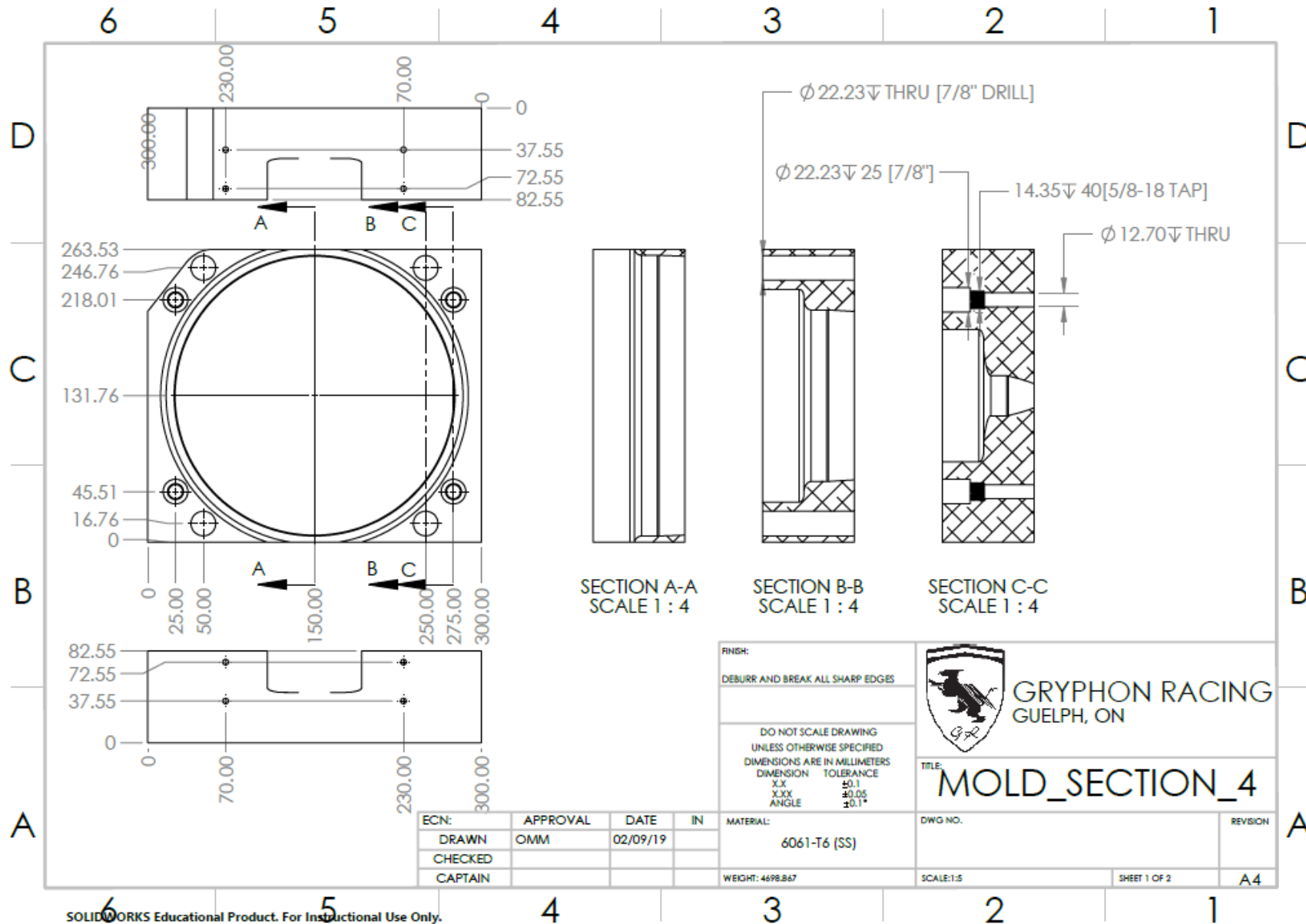
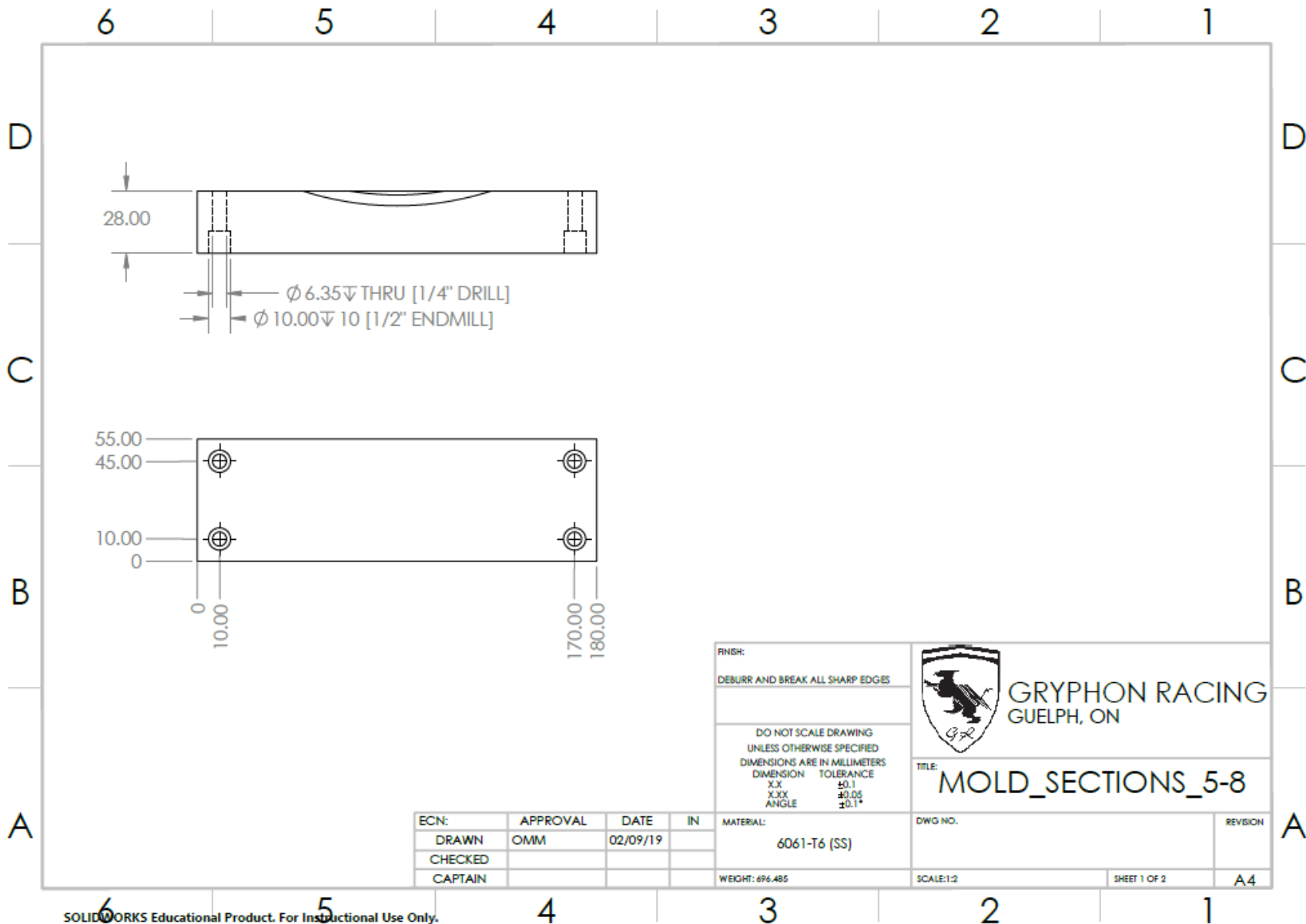


Figure 51: Drawing for Mold Section 3



SOLIDWORKS Educational Product. For Instructional Use Only.

Figure 52: Drawing for Mold Section 4



## 7.0 RESOURCES

---

### People

Barry Verspagen – SOE Mechanical Technologist: Assisted the group in coordinating CNC machining in the AML, as well as tensile testing in the Material Science lab.

Ken Graham – SOE Machinist: Provided general machining advice.

Dave Wright – SOE Machinist: Provided general machining advice.

Anthony Meola – Gryphon Racing Design Lead: Consulted with group to assist in planning of carbon layup process.

### Software

MATLAB – Used for building tire data processing programs.

SOLIDWORKS – Used for solid modeling of rims and mold assembly.

ANSYS – Used for performing FEA of Aluminum and Carbon Rims.

MasterCAM – Used for programming CNC toolpaths.

Microsoft Word + Excel – Used for preparing documentation.

## 7.1 BILL OF MATERIALS AND EQUIPMENT

---

Mold				
Description	Quantity	Supplier	Part #	Notes
1/2" Socket Head Shoulder Bolts	8	Fastenal	26358	3" shoulder length, 3/8"-16 thread. Used for fastening main mold sections.
1/2" Socket Head Shoulder Bolts	4	Fastenal	26356	2.5" shoulder length, 3/8"-16 thread. Used for fastening main mold sections.
1/4" Socket Head Bolts	16	Fastenal	11587951	1" length, 1/4"-20 thread. Used for fastening sections 5-8 onto main sections.
Aluminum Block: 300x265x100	1	Gryphon Racing	N/A	Section 1. Outside shell of the rim. 6061-T6 Aluminum.
Aluminum Block: 300x265x45	1	Gryphon Racing	N/A	Section 2. Bottom face of both outside and inside of rim. 6061-T6 Aluminum.
Aluminum Block: 300x265x70	1	Gryphon Racing	N/A	Section 3. Mold 1 of 2 for outside shell. 6061-T6 Aluminum.
Aluminum Block: 300x265x85	1	Gryphon Racing	N/A	Section 4. Mold 2 of 2 for outside shell, includes Bead. 6061-T6 Aluminum.
Aluminum Block: 180x55x30	4	Gryphon Racing	N/A	Section 5-8. Added mold to provide easy handling and accommodation

				of wider rims around tire beads. 6061-T6 Aluminum.
<b>Rim</b>				
Description	Quantity (each rim)	Supplier	Part #	Notes
Aeropoxy PR 2032 Resin and PH 3663 Hardener	0.22 kg	Canada Composites	AE2032-63-X	High performance epoxy laminating resin used for demanding structural applications
2x2 Twill Weave Carbon Fibre	0.23 kg	Gryphon Racing	N/A	Carbon fibre with a 2x2 weave, adding flexibility to accommodate a wider range of geometries.
<b>Equipment</b>				
Description	Quantity	Location	Part #	Notes
Bandsaw	1	University of Guelph Machine Shop	N/A	For rough shaping of aluminum blocks.
Manual Mill	1	University of Guelph Machine Shop	N/A	For the majority of manual work done on molds
CNC Machine	1	University of Guelph Machine Shop	N/A	For work that is too precise or time-consuming for manual machining
Manual Lathe	1	University of Guelph Machine Shop	N/A	Machining of mold release bolts
Vacuum Pump	1	Gryphon Racing Shop	N/A	Maintains vacuum during carbon fibre setting
CNC router	1	Gryphon Racing Shop	N/A	For machining molded carbon fibre parts